



Wisconsin Geological and Natural History Survey
3817 Mineral Point Road
Madison, Wisconsin 53705-5100
TEL 608/263.7389 FAX 608/262.8086
www.uwex.edu/wgnhs/

James M. Robertson, Director and State Geologist

Mechanisms of groundwater flow across the Maquoketa Formation

David Hart
Ken Bradbury
Daniel Feinstein
Basil Tikoff

2008

Open-File Report 2008-03

This report represents work performed by the Wisconsin Geological and Natural History Survey or colleagues and is released to the open files in the interest of making the information readily available. This report has not been edited or reviewed for conformity with Wisconsin Geological and Natural History Survey standards and nomenclature.

Mechanisms of Groundwater Flow across the Maquoketa Formation

by
David Hart¹, Ken Bradbury¹, Daniel Feinstein², and Basil Tikoff³

- 1. Wisconsin Geological and Natural History Survey, University of Wisconsin-Extension**
- 2. United States Geological Survey-Wisconsin District**
- 3. Department of Geology & Geophysics, University of Wisconsin-Madison**

Final Report submitted to Wisconsin Groundwater Research Program at completion of grant number 144-NP30.

Title: *Mechanisms of Groundwater Flow across the Maquoketa Formation*

Project I.D.: *WDNR Groundwater Research Program 144-NP30*

Investigators: *David Hart (PI), Associate Professor, Wisconsin Geological and Natural History Survey, University of Wisconsin-Extension*
Kenneth Bradbury (Co-PI), Professor, Wisconsin Geological and Natural History Survey, University of Wisconsin-Extension
Daniel Feinstein (Co-PI), Hydrogeologist, United States Geological Survey-Wisconsin District
Basil Tikoff (Co-PI), Associate Professor, Department of Geology and Geophysics, University of Wisconsin-Madison.
Suzanne Braschayko (Project Assistant), Wisconsin Geological and Natural History Survey, University of Wisconsin-Extension
Jeff Wilcox (Project Assistant), Department of Geology and Geophysics, University of Wisconsin-Madison

Period of Contract: May 1, 2005 to June 30, 2006

Background/Need: Groundwater use in southeastern Wisconsin has resulted in more than 400 feet of drawdown in the deep sandstone aquifer since pumping began in the 1860's. Because of this drawdown, the area was designated as a critical groundwater management area in the 2003 Groundwater Protection Act 310. The deep sandstone aquifer is confined by a regional aquitard, the Maquoketa Formation, over much of southeastern Wisconsin. This aquitard is important because it controls how much water can enter the deep sandstone aquifer. Currently pumping from the deep sandstone aquifer is 33 million gallons per day. Of this amount, around 8 mgd is estimated to flow downward across the Maquoketa Formation through poorly understood pathways.

Objectives: We sought to understand how groundwater is flowing across the Maquoketa Formation, whether through multiaquifer wells or the Waukesha fault.

Methods: We conducted two simultaneous investigations to determine whether significant flow can occur through multiaquifer wells or the Waukesha fault. Our hypotheses and approach to testing them are below.

Possibility 1: Significant flow moves downward through cross-connecting multiaquifer wells. Our approach to explore this possibility included: 1) A records search to identify the number and location of multiaquifer wells in southeastern Wisconsin. 2) A review of well abandonment history to determine how many of these wells still exist. 3) Simulation of the wells using a numerical flow model. 4) A sensitivity analysis to determine the potential importance of the existing wells to the regional flow system.

Possibility 2: Significant flow moves downward along the Waukesha fault. Our approach to explore this possibility included: 1) A literature review of the Waukesha fault and the tectonic setting of the Michigan Basin. 2) A field visit to a quarry exposure of the Waukesha fault and other joints and fractures. 3) Incorporation of the Waukesha fault into a regional groundwater flow model. 4) Sensitivity analysis to determine the potential importance of the fault to the regional flow system. 5) Rehabilitation of borehole WK-1376 to allow study of the horizontal fractures through the Maquoketa Formation.

Results and Discussion:

We found there are more than 100 multiaquifer wells in southeastern Wisconsin. The simulated flow through these multiaquifer wells is currently estimated to be 4.4 mgd. Model calibration at higher flows is not possible without adjusting hydrologic parameters outside of reasonable bounds. Simulated flows through the multiaquifer wells are not evenly distributed. Few high flow wells contribute the majority of flow. Increased drawdown due to abandonment of the multiaquifer wells will be small because the flow rate of 4.4 mgd is only 15 percent of the total pumped from the deep sandstone aquifer and because many of the wells may never be located for abandonment.

Flow through the Waukesha fault system was investigated. If low estimates of the fault hydraulic conductivity of 5.6×10^{-3} ft/day are used, then the Waukesha fault plays a relatively unimportant role in the larger flow system. If the fault hydraulic conductivity is closer to an upper estimate of 0.28 ft/day, the flow through the Waukesha fault of around 4 mgd is similar in magnitude to that through the multiaquifer wells. As was the case with the multiaquifer wells, model calibration at higher flows is not possible without adjusting hydrologic parameters outside of their reasonable bounds. While the flow value of 4 mgd is significant, it does not represent the majority of flow across the Maquoketa Formation. We suspect that many smaller unmapped faults, fractures and joints contribute to flow across the Maquoketa Formation.

**Conclusions/
Implications/**

Recommendations: Multiaquifer wells and the Waukesha fault may transmit significant flow through the Maquoketa Formation but they do not dominate the flow system. Rather we suspect many distributed joints and fractures transmit most of the flow through the Maquoketa Formation. The Waukesha fault might contribute significant flow if the hydraulic conductivity in the fault is dominated by fractures in a damaged zone through the Maquoketa Formation. Otherwise, the flow through the Waukesha fault likely is not significant and it is merely one of many fractures and joints that transmit water across the Maquoketa Formation.

We recommend the following:

- Continue abandonment of the multiaquifer wells to limit contamination to the deep sandstone aquifer.
- Additional observation wells should be placed in the deep sandstone aquifer. The calibration effort was hampered by a lack of water level observations at depth and areally across southeastern Wisconsin.
- Collect groundwater use data for high capacity active wells. Only 69 of the 172 multiaquifer wells had pumping records available.
- Continue tracking the status of the high capacity wells. Unreported and unabandoned wells may present unknown pathways for contaminants to enter the deep sandstone aquifer.

Related Publications:

Braschayko, Suzanne (2005) The Waukesha Fault and Its Relationship to the Michigan Basin: A Literature Compilation. Wisconsin Open File Report 2005-05, Wisconsin Geological and Natural History Survey, Madison, WI. pp 62.

Key Words:

Multiaquifer wells, Maquoketa Formation, aquitards, Waukesha fault,

Funding: WDNR Groundwater Monitoring and Research Program Grant Number 144-NP30.

Final Report: A final report containing more detailed information on this project is available for loan at the Water Resources Institute Library, University of Wisconsin - Madison, 1975 Willow Drive, Madison, Wisconsin 53706 (608) 262-3069.

Table of Contents

Table of Contents	2
List of Figures	3
Introduction and Background	4
Project Approach	6
Multiaquifer Wells	6
Introduction	6
Flows through multiaquifer wells	7
Multiaquifer well locations and historical records in Southeastern Wisconsin	12
Multiaquifer wells and the regional groundwater flow model	14
<i>Effects of multiaquifer wells on the regional flow system</i>	14
<i>Sensitivity of the model solution to various parameters</i>	17
<i>Limitations of Data and the MNW Package with Regard to the Regional Flow Model</i>	22
<i>Best model results</i>	22
Summary	24
Flow through joints and faults	25
Introduction	25
Waukesha fault	25
<i>Waukesha Fault Quarry Description</i>	26
<i>Waukesha Fault and regional groundwater flow model</i>	28
<i>Waukesha Fault Summary</i>	31
Other Faults and Joints	32
Redevelopment of the Pewaukee Corehole	34
Summary	37
Recommendations	38
References	39

List of Figures

- Figure 1. Regional Hydrostratigraphy of Southeastern Wisconsin.
- Figure 2. Drawdown in the deep sandstone aquifer.
- Figure 3. Diagram showing how flows through multiaquifer wells can be calculated.
- Figure 4. Locations of spinner flow logs showing significant multiple-aquifer flow.
- Figures 5a, b, and c. Borehole and flow logs for wells VN-239, DN-1495, and WK-37.
- Figure 6. Locations and status of multiaquifer wells in southeastern Wisconsin.
- Figure 7. Histogram of the number of multiaquifer wells over time.
- Figure 8. Comparison between the base model and the base model with multiaquifer wells.
- Figure 9. Calibration curves of the base model and the base model with multiaquifer wells.
- Figure 10. Model comparisons of residual means and absolute residual means.
- Figures 11a and b. Flows through multiaquifer wells using combined multiaquifer well model.
- Figure 12. Histogram of present-day simulated downward flows in multiaquifer wells.
- Figure 13. Map showing location of the Waukesha fault traces.
- Figure 14. Air photo of the quarry.
- Figure 15. Photo of the Waukesha fault at the Waukesha Stone and Lime Quarry.
- Figure 16. Photo of fractures in the upper Maquoketa Formation.
- Figure 17. Joint in the east quarry of the Waukesha Lime and Stone Quarry.
- Figure 18. Cuttings showing ground-up packer.
- Figure 19. Water levels in the buried piezometer nest.
- Figure 20. The effect of an aquitard in a regional flow system.

Introduction and Background

Aquitards provide barriers to contaminants on one hand while limiting recharge to aquifers on the other. Understanding the pathways through aquitards that allow contaminants and recharge to enter an adjacent aquifer is essential for protection of the aquifer and quantifying the groundwater flow system. Flow across aquitards can occur through different pathways, e.g., the porous matrix of the aquitard, erosional or depositional windows, fractures, and multiple aquifer wells. Identifying the dominant flow mechanism is difficult but important for characterization of the aquitard.

We investigated flow across a regional aquitard in southeastern Wisconsin, the Maquoketa Formation with attention to flow through multiaquifer wells and the Waukesha fault system. The Maquoketa Formation is predominantly shale with interbedded dolomite. Where present to the east, this aquitard separates a shallow glacial and dolomite aquifer from a deep sandstone aquifer. This hydrostratigraphy is shown in Figure 1.

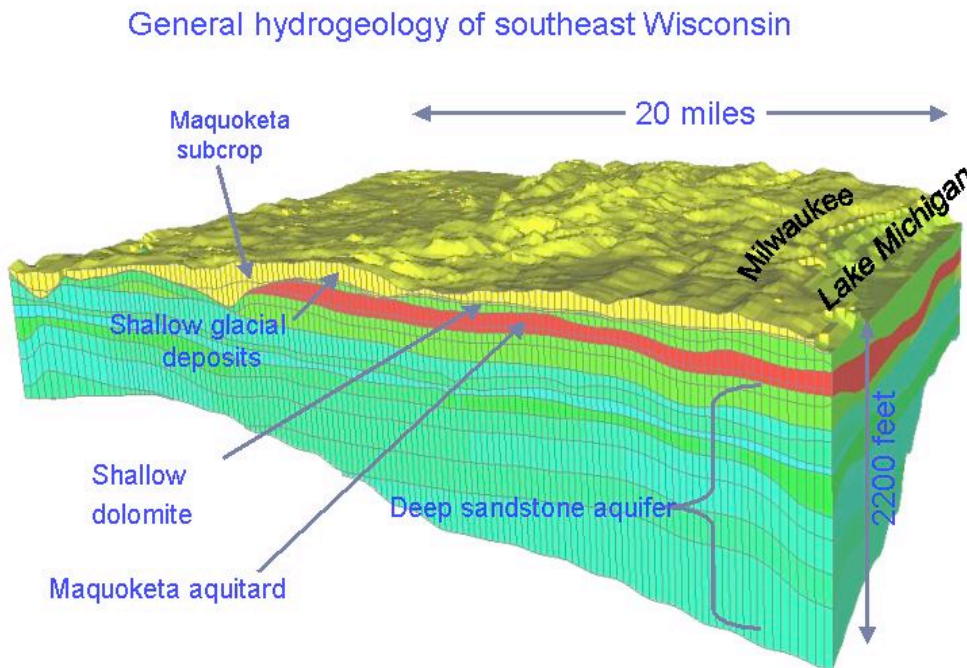
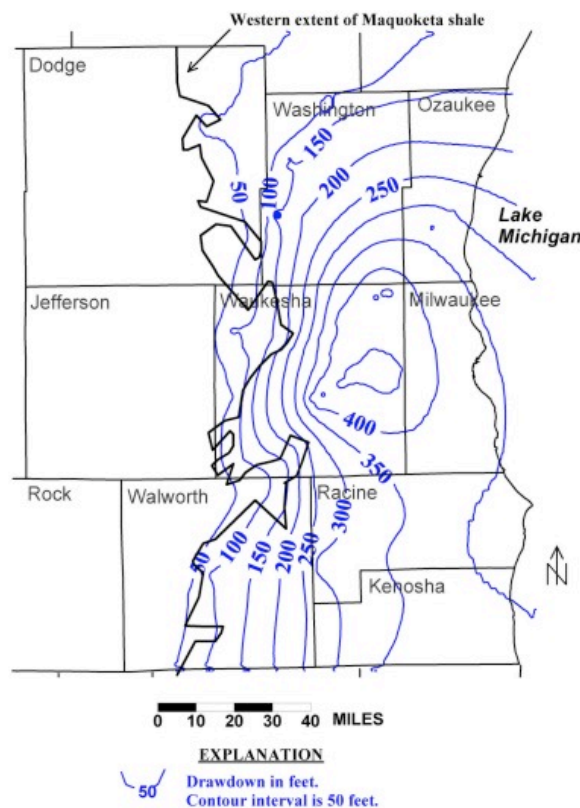


Figure 1. Regional Hydrostratigraphy of Southeastern Wisconsin.

A regional cone of depression has formed beneath the Maquoketa Formation in the deep sandstone aquifer. More than 400 feet of drawdown has occurred in the sandstone aquifer since

1860 with an additional 7 feet of additional drawdown occurring every year in some areas. This drawdown is driven by ever increasing pumping rates that have doubled every 50 years since pumping began in the 1860's. A regional groundwater model (Feinstein and others, 2005) includes pumping of 33 million gallons per day (mgd) of groundwater from the deep sandstone aquifer. The model predicts that while the main source of replenishment is to the west where the Maquoketa is not present, approximately 25 percent of that flow (8 mgd) is crossing the Maquoketa Formation into the regional cone of depression to replenish the pumped water. Figure 2 shows the extent of the regional cone of depression and its relation to the Maquoketa Formation.



Drawdown in Deep Sandstone (St Peter) from 1864 to 2000

Figure 2. Drawdown in the deep sandstone aquifer (Feinstein and others, 2005). The dark line is the western most extent of the Maquoketa Formation.

Calibration of a regional groundwater flow model for southeastern Wisconsin (Feinstein and others, 2005) suggested that the regional vertical hydraulic conductivity (K_v) of the Maquoketa Formation is 1.8×10^{-11} m/s (5×10^{-6} ft/day) while core-scale measurements range from 2.5×10^{-14} to 1.4×10^{-12} m/s (7×10^{-9} ft/day to 4×10^{-7} ft/day) (Hart and others, 2005). Flow through some additional pathways in the shale might explain the apparent increase of bulk K_v at the

regional scale. Based on well logs, erosional windows or high conductivity zones with no shale do not seem to be present east of the Maquoketa Formation subcrop. Instead, we believe that discrete features, either fractures or open boreholes, cause the higher Kv at the regional scale.

Project Approach

We conducted two simultaneous investigations to determine whether significant flow can occur through multiaquifer wells or, specifically the Waukesha Fault system. Our hypotheses and approach to testing them are below.

Possibility 1: Significant flow moves downward through cross-connecting multiaquifer wells.

Our approach to explore this possibility included:

- A records search to identify the number and location of multiaquifer wells in southeastern Wisconsin.
- A review of well abandonment history to determine how many of these wells still exist.
- Simulation of the wells using a numerical flow model.
- A sensitivity analysis to determine the potential importance of the existing wells to the regional flow system.

Possibility 2: Significant flow moves downward along the Waukesha fault. Our approach to explore this possibility included:

- A literature review of the Waukesha fault and the tectonic setting of the Michigan Basin.
- A field visit to a quarry exposure of the Waukesha fault and other joints and fractures.
- Incorporation of the Waukesha fault into a regional groundwater flow model.
- Sensitivity analysis to determine the potential importance of the fault to the regional flow system.
- Rehabilitation of borehole WK-1376 to allow study of the horizontal fractures through the Maquoketa shale.

Multiaquifer Wells

Introduction

Multiaquifer wells are wells that are open to several aquifers separated by aquitards. The open well provides a pathway from one aquifer to the next. If a hydraulic gradient is present between the aquifers, water will flow out of one aquifer through the well into another aquifer.

These wells can significantly increase flow across aquitards to the point of being the predominant method of transport across an aquitard if enough wells are present.

Flows through multiaquifer wells

Flow through multiaquifer wells is dependent on several factors illustrated in Figure 3. These factors include the transmissivities and heads of the contributing and receiving aquifers, the multiaquifer well radius, and any well bore losses or friction effects in the well. The well bore flow across an aquitard can be calculated using coupled steady state Theim equations and mass balance between the aquifers. The MODFLOW MNW package (Halford and Hanson, 2002) uses this same scheme within MODFLOW's finite difference cells. The composite head in the well and flow through the well are calculated using the two aquifer heads, thicknesses, and hydraulic conductivities. The radius of the well and the radius of influence are also needed as inputs. Figure 3 shows sample inputs and the coupled Theim equations. If we use the values shown in Figure 3 and a far field radius of 10,000 feet, we can solve the equations in Figure 3 for flow in the well, Q . The result is around 150 gpm for an 8" diameter well. This method would overestimate flow through a real well because it does not include friction or well bore loss effects.

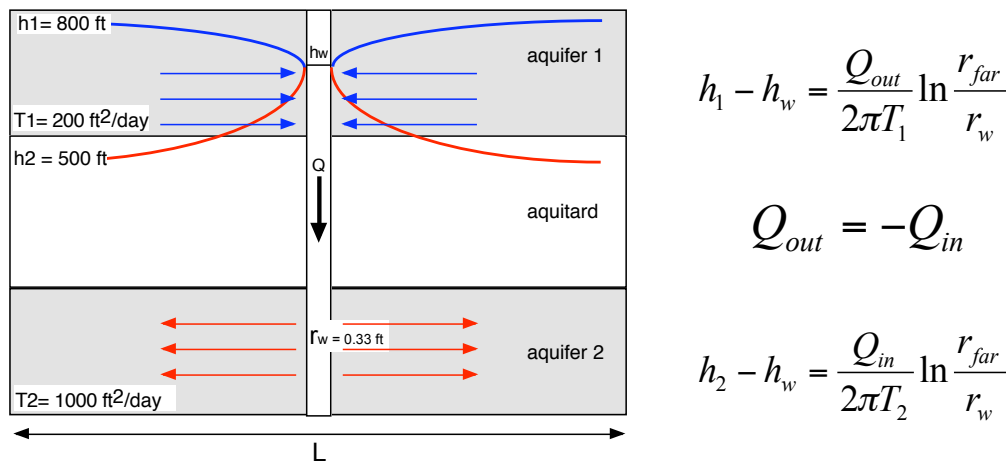


Figure 3. Diagram showing how flows through multiaquifer wells can be calculated.

To check this calculation of theoretical flow, we measured the multiaquifer flows in three wells, VN-239, DN-1495, and WK-37. Only one of those wells is located in southeastern Wisconsin. The other two wells are located in southern and southwestern Wisconsin but are of similar construction and depth as many of the multiaquifer wells in southeastern Wisconsin. The

locations of the three wells that were logged are shown in Figure 4. Other candidates for logging in southeastern Wisconsin were found to be either abandoned or in use and so not available. We hope to measure these wells as they become available for logging. Figures 5a, 5b, and 5c show the geology, geophysical logs, and flow logs of these wells. We measured maximum downward flows in the absence of pumping of 90, 60, and 80 gallons per minute in wells, VN-239, DN-1495, and WK-37, respectively, using a spinner flow meter. Increasing downward flow is shown on the plots as more negative. An increase in downward flow shows the adjacent formation is contributing water to the well. A decrease shows that the adjacent formation is receiving water.

Significant measured flow can occur in multiaquifer wells in the absence of any pumping, both through fracture and porous media flow. The flow into well VN-239, Figure 5a, was dominated by a single fracture 0.5 meter wide at a depth of 32 meters. Some flow out of the well occurred in the Tunnel City Group but most of the outflow occurred in the Wonewoc sandstone. This well has since been reconstructed and is no longer a multiaquifer well. In contrast, the flow into well DN-1495, Figure 5b, was porous media flow. It was evenly distributed throughout the lower section of the Tunnel City Group and the entire section of Wonewoc. The outflow in this well was evenly distributed throughout most of the Mount Simon sandstone. In the last example, WK-37, Figure 5, the water was reported as audibly cascading into the well. The spinner log shows flow at a maximum in the Maquoketa shale, with a slight decrease below the shale showing some outflow there. Most of the outflow in this well must occur beneath the logged portion of the well in the Mount Simon sandstone. The total depth of this well is 1300 feet and is not shown in the log.

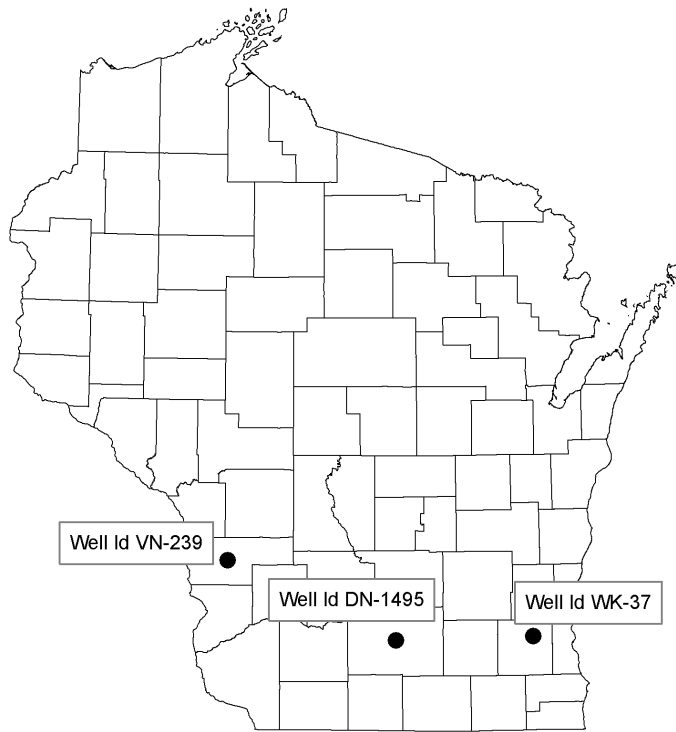


Figure 4. Locations of spinner flow logs showing significant multiple-aquifer flow.

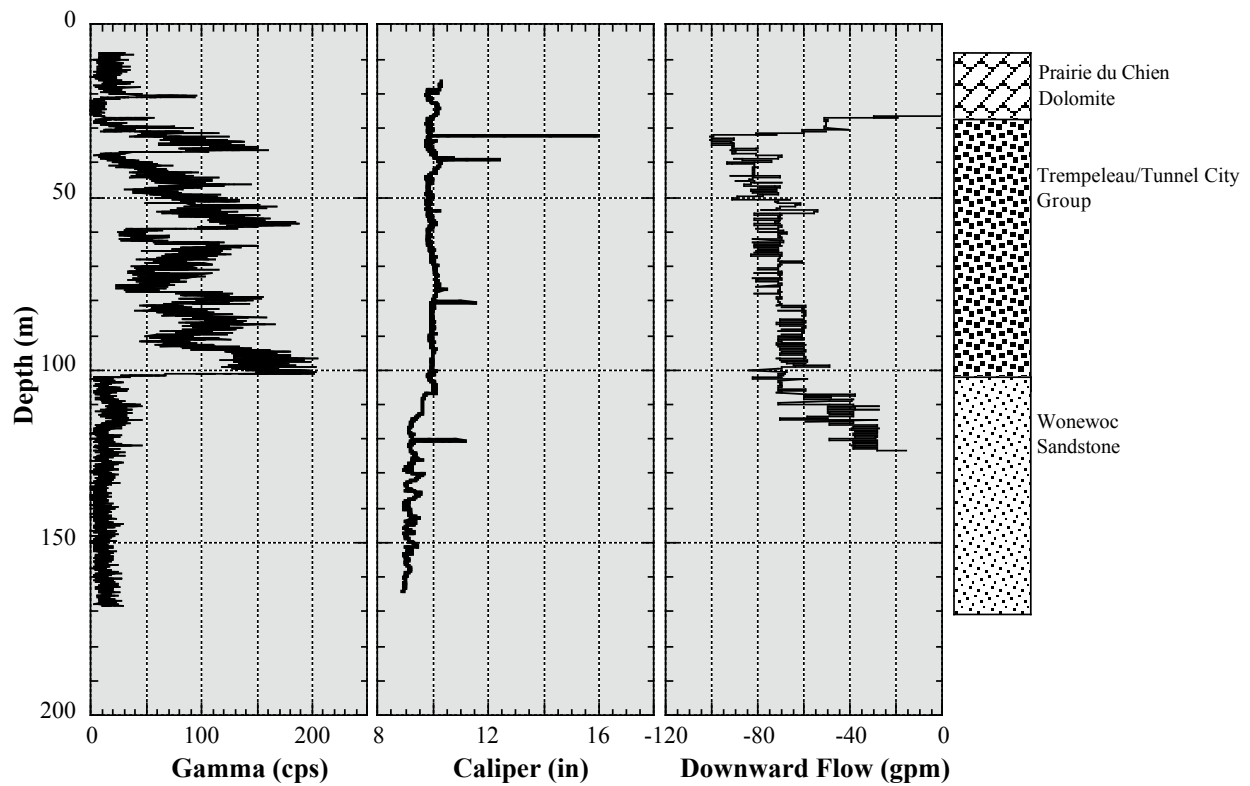


Figure 5a. Well VN-239, located near Viroqua, WI. The upper aquifer is the Prairie du Chien dolomite. The aquitard is the base of the Prairie du Chien or the top of the Tunnel City Group. The lower aquifer is the Tunnel City group and the Wonewoc sandstone. Increasing downward flow is shown as more negative. This well has since been reconstructed and is no longer a multiaquifer well.

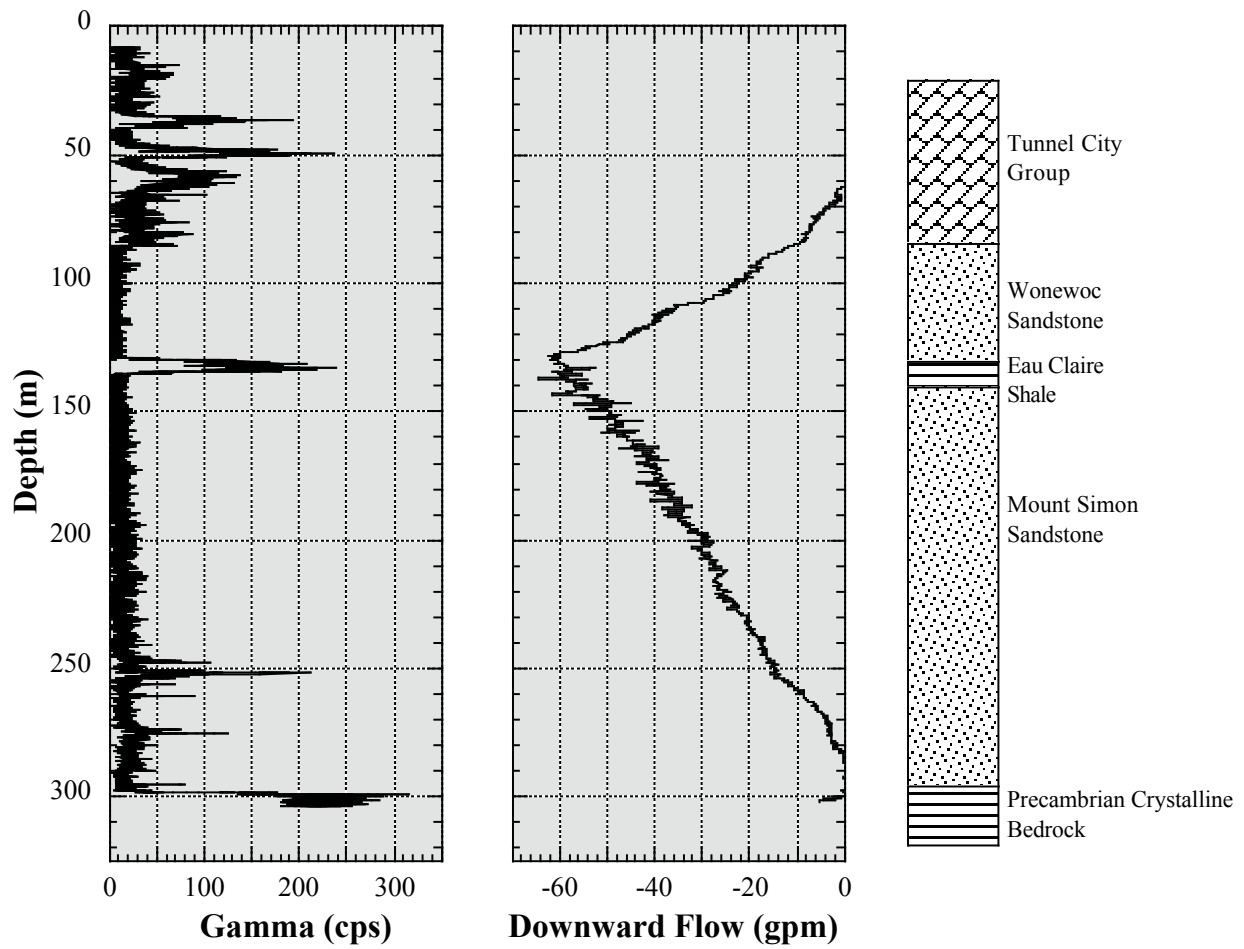


Figure 5b. Well DN-1495, located near Madison, WI. The upper aquifer is the Tunnel City Group and the Wonewoc sandstone. The aquitard is the Eau Claire shale. The lower aquifer is the Mount Simon sandstone. Increasing downward flow is shown as more negative.

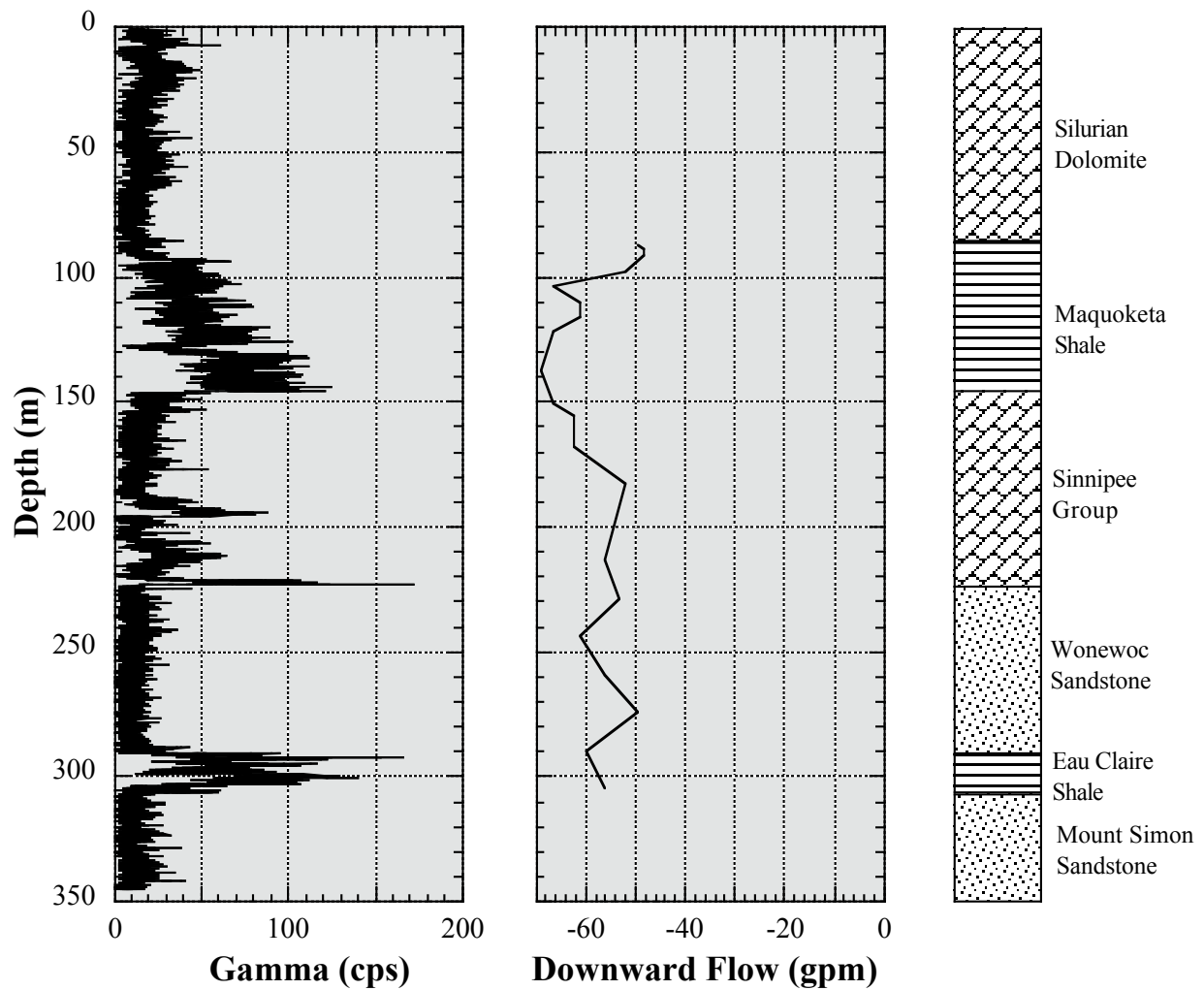


Figure 5c. Well WK-37, located near Pewaukee, WI. The upper aquifer is the Silurian dolomite. The aquitard is the Maquoketa shale and Sinnipee Group. The lower aquifer is the St Peter/Wonewoc sandstones undifferentiated and the Mount Simon sandstone. The well extends to a total depth of 1500 feet, not shown in the log. Increasing downward flow is shown as more negative.

Multiaquifer well locations and historical records in Southeastern Wisconsin

The number and locations of multiaquifer wells must be known to test whether or not they have a significant impact to the groundwater flow system in southeastern Wisconsin. We conducted a search of the WGNHS well database, WiscLith. That search identified 172 wells

that were located in southeastern Wisconsin and penetrated the Maquoketa formation with open intervals above and below the Maquoketa formation at some time. We then joined available pumping records with the identified multiaquifer wells. We found pumping records for only 69 of the 172 multiaquifer wells. In addition to identifying when the well was constructed from the WiscLith database, we also searched available well abandonment forms at the local DNR offices. That information allowed us to determine the time interval of possible multi-aquifer flow for a particular well.

Most of the multiaquifer wells in southeastern Wisconsin are located in the eastern counties, with Milwaukee County having the most wells (Figure 6). The status of the majority of wells is “still present, use unknown”. We do not know if these wells are actively used, abandoned, or merely inactive. Only a few multiaquifer wells are listed by the WDNR as active. The WDNR office in Milwaukee County has taken a more active stance to abandon multiaquifer wells. As a result, the majority of abandoned wells are located there. Figure 7 is a histogram showing the number of multiaquifer wells over time. The number peaked at 162 wells between 1985 and 1990. Since then, some wells have been abandoned and currently there are 133 multiaquifer wells. The majority of the unabandoned multiaquifer wells are not municipal, but were once owned and operated by industry.

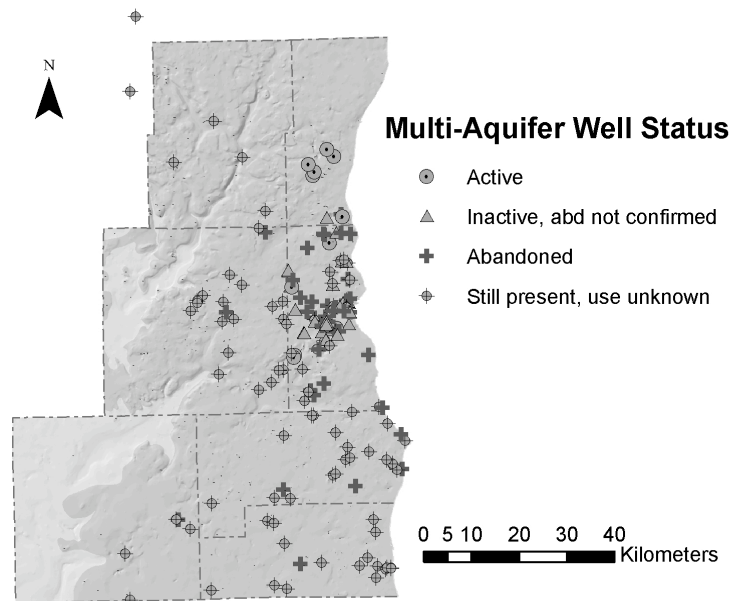


Figure 6. Locations and status of multiaquifer wells in southeastern Wisconsin.

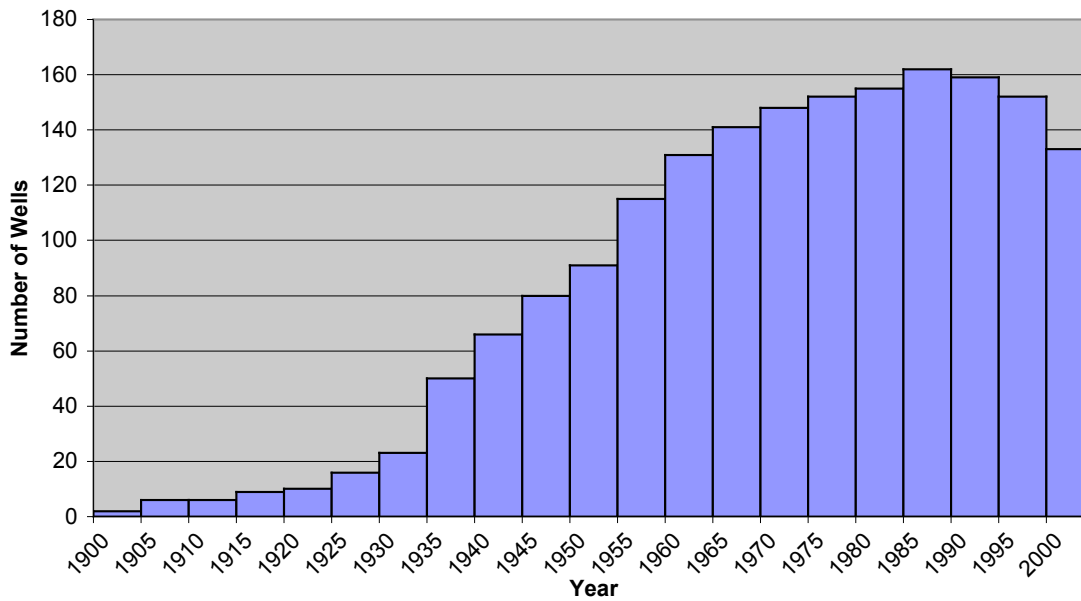


Figure 7. Histogram of the number of multiaquifer wells over time.

Multiaquifer wells and the regional groundwater flow model

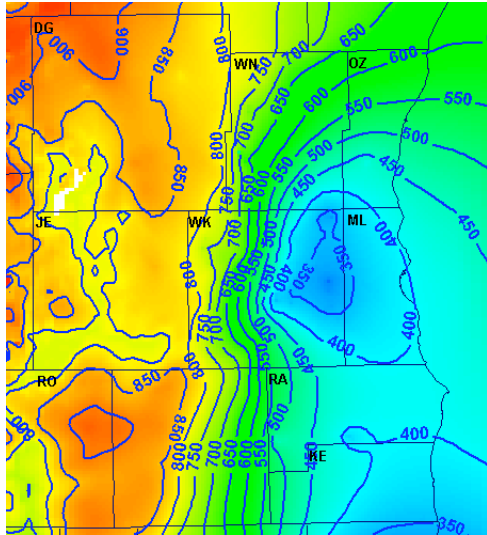
We investigated the role of multiaquifer wells in the regional groundwater flow system using the regional groundwater flow model for southeastern Wisconsin (Feinstein and others, 2005). We used the multimode well (MNW) package (Halford and Hanson, 2002) to simulate the flow through the multiaquifer wells. We first ran the model with the multiaquifer wells and compared that result to the base model. We then conducted a sensitivity analysis to determine which multimode well parameters most affected the model results. Following the sensitivity analysis, we arrived at a model that included the multiaquifer wells and matched the head targets reasonably well. However, that model did not have a better fit to the targets than the base model that did not include the multiaquifer wells. The limitations we discovered during the sensitivity analysis prevented a more complete calibration. We concluded the effort by calculating flows across the aquifer using the best-fit model that incorporated the multiaquifer wells.

Effects of multiaquifer wells on the regional flow system

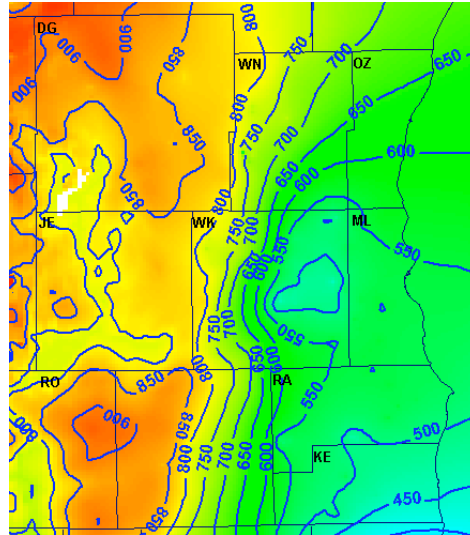
Given the number of multiaquifer wells and the measured flow in the three multiaquifer wells, it seems likely that these wells have altered the flow system in southeastern Wisconsin. There are more than 100 multiaquifer wells in southeastern Wisconsin and flows of more than 50 gallons per minute have been measured in similar multiaquifer wells. A simple multiplication of

100 wells x 50 gpm/well gives a rough estimate of 5000 gpm (7.2 million gallons per day). While this is an overestimation, it suggests that multiaquifer flow is an important component of flow through the Maquoketa shale when compared to the calibrated regional model result of 8 million gallons per day flow across the Maquoketa. This simple calculation can be used to determine whether or not further investigations of multiaquifer wells should occur in other regions.

We incorporated the multiaquifer wells into the regional aquifer model using the MNW package. Each well was included into the model only during the stress during which it was installed until the stress period during which it was abandoned. If pumping rates were available, they were included in the corresponding model stress period. The open interval of each well was associated with the corresponding model layers. We compared model results from the calibrated base model to the model including the multiaquifer wells. As predicted by the calculation above, the multiaquifer well model result shows significant flow across the Maquoketa through the multiaquifer wells. Figure 8 shows a comparison of the heads in the St. Peter sandstone between the two models. The base model has a cone of depression located in Waukesha County (WK) with heads of 350 feet above sea level. When the multiaquifer wells are included in the model, the cone of depression is still located in the same position in Waukesha County but the drawdown is much less. The water levels in this simulation are 500 feet above sea level. The additional flow through the multiaquifer wells gives a simulated increase in water levels in the deep aquifer of more than 150 feet.



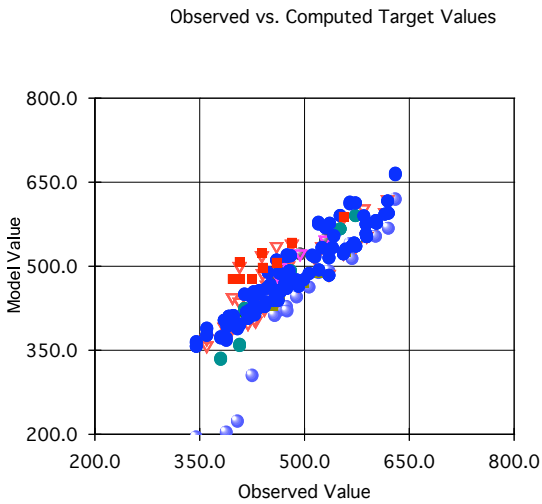
Base Model



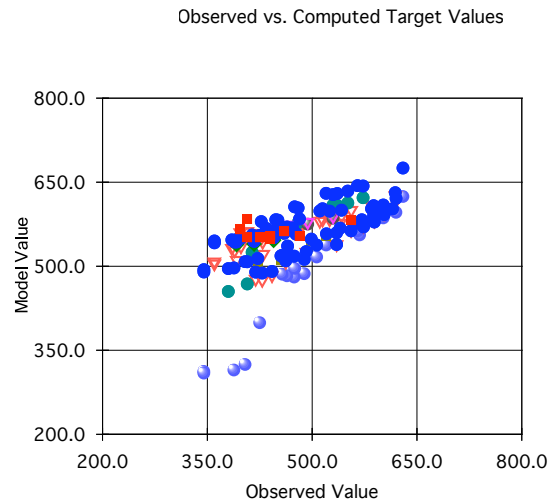
Base Model with multiaquifer wells

Figure 8. Comparison between the base model and the base model with multiaquifer wells for Year 2000 water levels in St. Peter Formation.

The model calibration was no longer within an acceptable range after including the multiaquifer wells. Figure 9 is a comparison between the calibrations of the base model and the model with multiaquifer wells. The base model calibration shows a relatively good one-to-one correlation between the modeled and target heads. The base model with the multiaquifer wells is noticeably biased. The model values are nearly always greater than the observed target values and lie above the one-to-one line of correlation. The variance of the residuals when the multiaquifer wells were included is also much larger than in the base model. The larger spread about the one-to-one correlation in the base model with multiaquifer wells plot shows this.



Base Model



Base Model with multiaquifer wells.

Figure 9. Comparison of calibration curves between the base model and the base model with multiaquifer wells over times that the target values were available.

We next investigated why inclusion of the multiaquifer wells caused the model calibration to significantly worsen. A possible explanation is that the base model does not represent actual conditions and recalibration of the model with the multiaquifer wells is necessary. Alternatively, the flows through the multiaquifer wells might be grossly overestimated by the model and MNW package. Other mechanisms might also be important. For example, the number of multiaquifer wells might be overestimated because not all abandoned wells are reported. Also, friction losses and silting of these wells might limit flows to significantly less than the simulation showed. Last, the model MNW package may be overestimating flow. Initial tests of these hypotheses are investigated and discussed below.

Sensitivity of the model solution to various parameters

We attempted to adjust salient model parameters to improve the model calibration when the multiaquifer wells are included. The parameters were adjusted twice, once to likely reasonable bounds and then to limits of their reasonable bounds based on available, independent sources and references. We adjusted the following hydrogeologic model parameters: the horizontal hydraulic conductivity (Kh) of the Silurian dolomite, the Kh of the deep sandstone aquifer, and the vertical hydraulic conductivity (Kv) of Maquoketa formation. We increased the pumping rates of the wells in the deep system to account for possible missing pumping and

increased the friction losses in the multiaquifer wells. Finally, we combined several of the parameter changes to give a “best fit” combined model that includes the multiaquifer wells. Figure 10 shows two calibration statistics for these model runs, the residual mean and the absolute residual mean. The target data used to fit the model was from 10 wells open to the deep sandstone aquifer with recorded water levels from the period between 1940 and 2000. The residual mean shows whether or not there is global bias in the model results. A negative residual mean corresponds to the model overestimating the heads in the deep sandstone aquifer, a positive residual mean corresponds to an underestimation. The absolute residual mean shows the magnitude of the residuals. A small absolute residual mean shows the model calculated heads are nearly equal to the measured head targets.

The base model has the best calibration statistics of all the models. It has a near-zero residual mean and the smallest residual mean of all the model runs. The model result when the multiaquifer wells are included is significantly worse. The multiaquifer well model overestimates nearly all of the head targets by around 70 feet.

We decreased the amount of water flowing down through the multiaquifer wells by decreasing the Kh of the Silurian by factors of 1/2 and then 1/10th in two model runs. In the base model, the Silurian dolomite was zoned into two Kh values of 4 and 1 ft/day. Both Kh values were decreased by the two factors. The midrange reasonable-multiplier of 1/2 was derived from the report by Dunning and others, 2004 in which they used a value of 0.6 ft/day for unweathered sections of the Silurian dolomite. The extreme range multiplier of 1/10 was derived from Rovey and Cherkauer, 1994. They reported slug test value ranges of 0.03 to 0.3 ft/day for the Mayville, Manistique, and Romeo Formations within the Silurian dolomite. The slug test values would likely scale up to larger values so the factor of 1/10 likely represents a lower reasonable bound for the regional Kh of the Silurian. The residual mean and the absolute residual mean are significantly reduced by changing this parameter within reasonable limits. Using the extreme range for the Kh of the Silurian (the factor of 1/10 of the base Kh) resulted in the second best model calibration that included multiaquifer wells.

We next decreased the Kv of the Maquoketa shale in two model runs by factors of 1/5 and 1/10. We decreased this unit from 5×10^{-6} ft/day to 1×10^{-6} ft/day for the midrange reasonable multiplier and from 5×10^{-6} ft/day to 5×10^{-7} ft/day for the lower limit. The midrange value was selected because it was at a lower limit that still allowed a good fit to the steady state model

(Hart and others, 2005). The lower limit of 5×10^{-7} ft/day has a significantly worse fit to the steady state model and is within the range of laboratory values of the Maquoketa, 1.2×10^{-6} – 5.1×10^{-9} ft/day (Hart and others, 2005). The model fit was not dramatically improved by these changes. The decrease from $1/5^{\text{th}}$ to $1/10^{\text{th}}$ of the base Kv caused little change in the calibration statistics. When the Maquoketa shale Kv is decreased beyond a certain point, flow through the multiaquifer wells dominates and so the Maquoketa Kv is no longer important to the model calibration.

A friction loss was applied to the multiaquifer wells. This was done to simulate silting or biofouling of the wells. Little guidance is available in the literature for application of this parameter. Discussions with the USGS and review of a USGS report (Hanson and others, 2002) suggest that a value of friction loss of 4 is a reasonable upper bound. This value of simulated friction loss corresponds to a decrease of the Kh around the well by a ratio of $K/K_{\text{friction}} = 6.7$ over a radius twice that of the well. The actual friction loss value is likely to be less than the one used here. This increase in friction loss has a significant effect on the model calibration as shown in Figure 10.

We also investigated the effects of partially penetrating multiaquifer wells. In the model, these wells were assigned to the entire model layer. That may have resulted in an overestimation of the transmissivity of the source and sink for the wells. A model run was conducted that truncated all partial layers so that the multiaquifer wells were placed only in those layers where they fully penetrated the entire layer. This model change had little effect and is not the prime error in the model. The mean absolute error changed from 79 to 68 ft as shown in Figure 10. A similar effect that was not tested was that some wells were abandoned during a stress period. These wells were left in the model for the entire stress period, with a resulting over estimation of flow.

As noted in Feinstein and others (2005), the pumping rates for the model might be underestimated by 9 million gallons per day (mgd), an increase of 13 %. We also noted that of the 172 multiaquifer wells, only 69 had associated pumping records. We averaged the pumping rate from the multiaquifer wells with pumping records and applied that rate to the multiaquifer wells with the missing pumping. The net increase in pumping was 3.5 mgd. We then distributed the difference between the 9 mgd and the 3.5 mgd to all the multiaquifer and single aquifer wells in the model. The resulting model run is shown as Pumping rate x 1.13 in Figure 10. This 13 %

increase in the pumping rate was the reasonable midrange change. An upper bound for the missing pumping (Gotkowitz, 2006) was set as an increase of 29% or 19.4 mgd. As before, 3.5 mgd was applied to the multiaquifer wells without pumping and the difference between the 19.4 mgd and 3.5 mgd was applied to all wells in the model. The resulting model run calibration statistics are shown as pumping rate x 1.29 in Figure 10. These changes do improve the model bias as shown by the low residual mean but still have relatively large spread as shown by the absolute residual mean.

The last parameter we varied was the deep sandstone Kh. The average value of the deep sandstone Kh was 2 ft/day. We ran two runs, one at 1.5 ft/day average Kh and 1 ft/day average Kh. These two values represent reasonable midrange and reasonable limits to the Kh as determined from the steady state model fit and pumping tests (Feinstein and others, 2005). The Kh of the deep sandstone aquifer is important for calibration of the model with multiaquifer wells as shown by the decrease in the residual mean and absolute residual mean as the Kh is reduced.

Last, we conducted a run that combined the midrange, reasonable parameter changes to the Kh of the Silurian, the friction losses in the well, the increased pumping rate, and a decrease in the deep sandstone Kh. In this combined run, the residual mean is positive as shown in Figure 10, meaning that the model heads are on average less than the target heads. The absolute residual mean is also significantly reduced, meaning that the spread about the head targets is reduced in this case. We used this model as the “best fit” model with multiaquifer wells. Additional calibration might improve the model fit but uncertainties in the pumping rates in the multiaquifer wells, the lack of constraint for the friction losses, and correlations between the Kh of the Silurian and Kh of the deep sandstones would result in non-unique models.

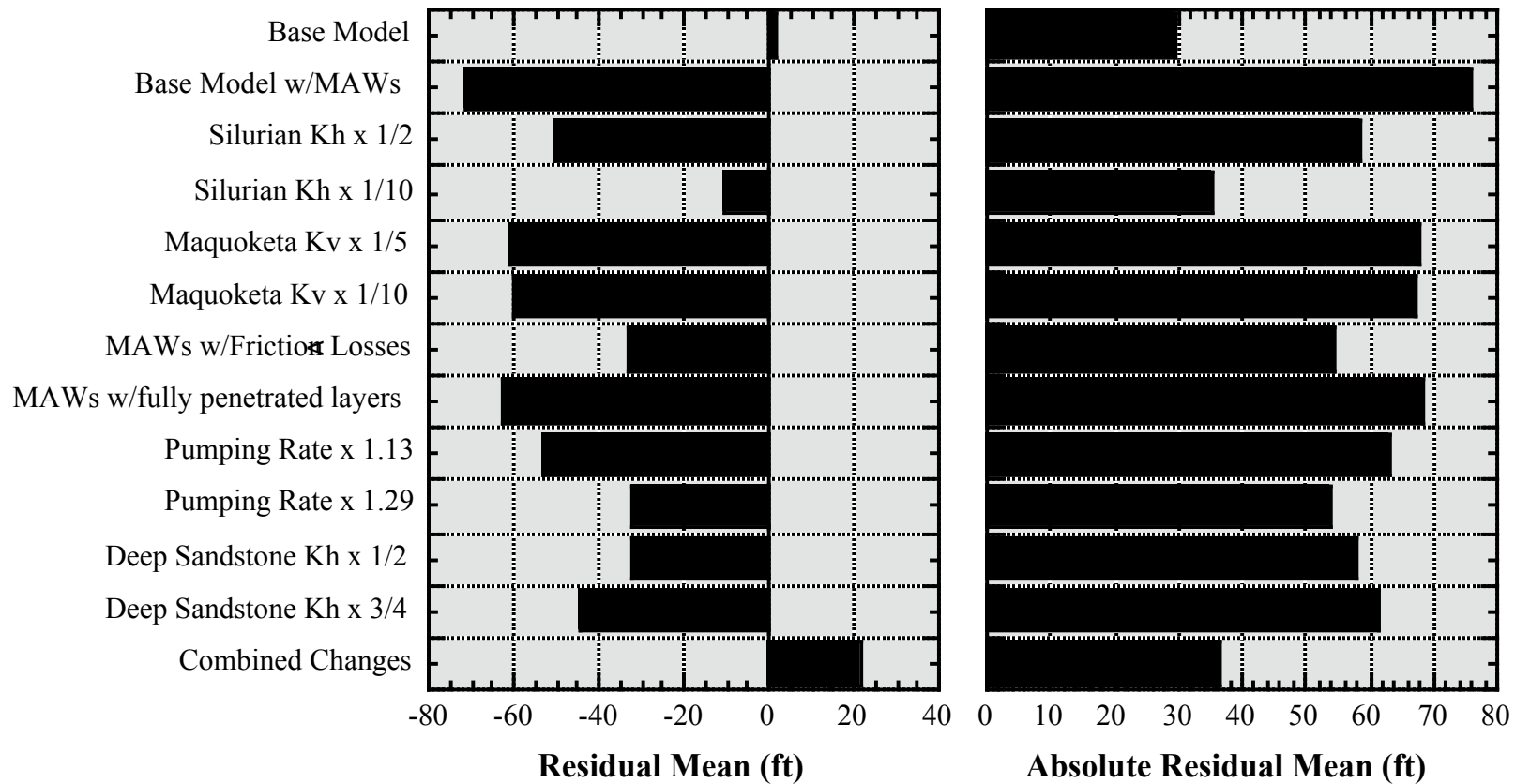


Figure 10. Model comparisons of residual means and absolute residual means.

Limitations of Data and the MNW Package with Regard to the Regional Flow Model

The model calibration is restricted by several factors. One of those factors is a lack of pumping records. Only 69 of the 172 multiaquifer wells have any pumping records associated with them. Few of these wells are municipal wells. Municipalities submit records of pumping to the Wisconsin Public Service Commission. Non-municipal wells are not required to submit such records. Another factor was that well abandonment is not always reported to the WDNR. Several wells were listed as “still active, status unknown” in the WDNR records but when the well owners were contacted, they reported the well to be abandoned.

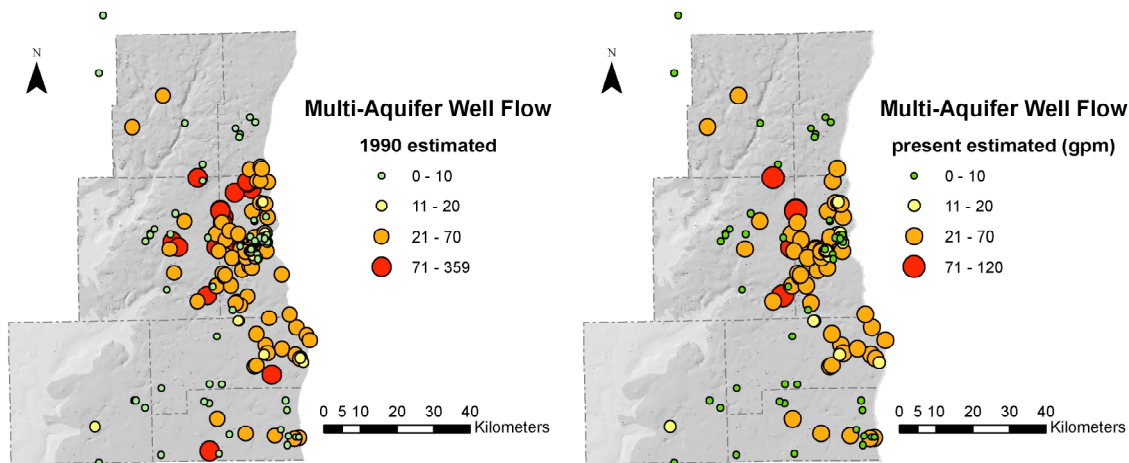
In addition to issues of record, the MNW package itself can misrepresent flow through a multiaquifer well. It can do this in two ways. The first error occurs when the upper aquifer is unconfined. The MNW package does not adjust for the formation of a seepage face but continues to apply the entire layer thickness to the calculation of the transmissivity. A second error arises when the water level in the well falls below the base of the upper aquifer. The hydraulic gradient is not limited to the difference between the head in the model cell and the elevation of the base of the aquifer but increases as the water level in the well drops. Both errors over-estimate flow. We shared these issues with the USGS developer of the MNW code and will continue to work with the USGS to improve the model package.

Best model results

We analyzed flows through the multiaquifer wells using the combined “best fit” model. Table 1 in Appendix A lists each of the multiaquifer wells that were present from 1990 to 2000 in southeastern Wisconsin. Many of the multiaquifer wells were abandoned between 1990 and 2000, the decade of the last model stress period. Figure 11a shows the multiaquifer wells present at the beginning of the stress period in 1990 and their flows at the end of the stress period. Figure 11b shows only those wells and their flows that were present during the entire stress period from 1990 to 2000. Many of the highest flow wells shown in Figure 11a were abandoned in that period. The flow into the deep sandstone aquifer, calculated from the combined model, decreases from 5.5 mgd to 4.4 mgd when the abandoned wells are removed from the total flow. The value of 5.5 mgd was likely an overestimate because of the model limitations listed above. Since the year 2000, additional higher flow multiaquifer wells have been abandoned so that now the flow through the multiaquifer wells is likely less than 4.4 mgd.

Although a lack of model targets, pumping records, and errors introduced by the modeling code prevent us from firmly stating how much flow is passing through these wells, this modeling effort suggests the multiaquifer well flow is significant. The model-predicted value of 4.4 mgd is around 15 percent of the total amount pumped from the deep sandstone aquifer. The total modeled flow from the shallow aquifer to the deep sandstone aquifer is increased by 50 percent from around 8 mgd to 12 mgd when the multiaquifer flow is added to the porous media flow.

Results of the combined model can be used to focus abandonment efforts on those wells that are allowing the most flow. There are five wells listed in Appendix A that have very high simulated flows (greater than 70 gpm). An additional 54 multiaquifer wells have high simulated flows (greater than 20 gpm). The combined flow of these 59 high and very high flow wells accounts for 88 percent of the total simulated flow. The other 66 wells not abandoned in 2006 account for only 12 percent of the total downward flow through multiaquifer wells. Figure 12 is a histogram showing the distribution of downward simulated flow. To reduce the effects of multiaquifer wells and potential to contaminate the lower aquifer, the 59 high and very high flow wells should be abandoned first. The wells are coded by shading in Table 1 in Appendix A with darker shades corresponding to higher flows.



Figures 11a and b. Flows through multiaquifer wells using combined multiaquifer well model.

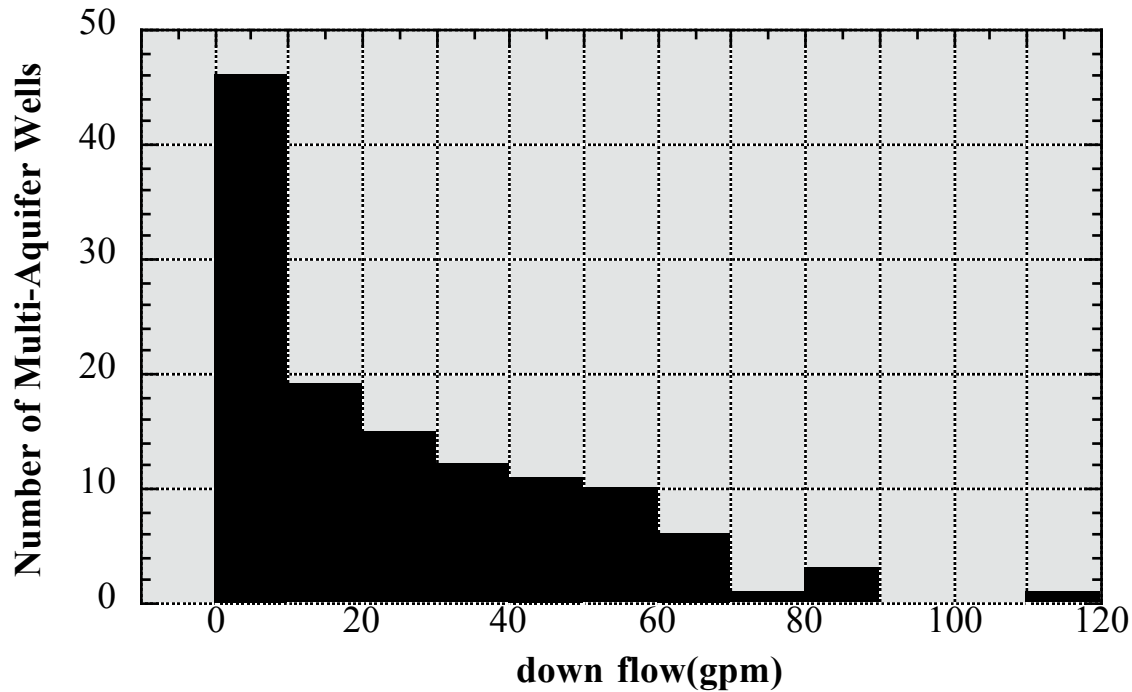


Figure 12. Histogram of present-day simulated downward flows in multiaquifer wells.

Summary

We conducted a database review of all the multiaquifer wells in southeastern Wisconsin. Those wells were placed in the regional groundwater flow model that allowed for multiaquifer flow. Inclusion of the multiaquifer wells into the base model resulted in an uncalibrated model. The simulated flow through the wells was larger than the model targets could allow. We conducted a series of model sensitivity runs by varying model parameters within reasonable bounds. We found it was not possible to bring the model back into calibration by varying a single parameter within reasonable limits. Rather, a combination of reasonable parameter changes gave a model that had a relatively good fit to the head targets. That model showed that the multiaquifer well flow to be around 4 mgd. That amount of flow is significant but not dominant within the flow system. Abandonment of multiaquifer wells may reduce flow into the deep sandstone aquifer, resulting in lower heads in the aquifer. That effect is offset by the risk posed to the deep sandstone aquifer by contaminants in the shallow aquifer transported through these wells.

Flow through joints and faults

Introduction

We investigated the role of the Waukesha fault in the regional groundwater flow system. It was postulated that this fault system allowed significant downward groundwater movement and that it might be a pathway for contaminant transport and recharge to the deep sandstone aquifer. We conducted a comprehensive literature review (Braschayco, 2005), made a site visit to the only known exposure of the Waukesha fault, and simulated the groundwater flows through the fault using the regional groundwater flow model.

Waukesha fault

The Waukesha fault system has been the subject of several studies that have identified it by offsets in geologic logs (Evans et al, 2004) and in the Waukesha Lime and Stone Company quarry in the Sinnipee dolomite near Waukesha, Wisconsin (Nelson, 1977), and by gravity and magnetic field studies (Sverdrup et al, 1997; and Skalbeck, 2006). The dip of the fault is near vertical in the quarry wall with an offset of 40 feet. However the gravity study by Sverdrup (1997) rejects a steeply dipping fault in favor of a shallow dip of 20 degrees or less with an offset of more than 1000 feet. It is possible that the fault is a listric growth fault with a near vertical dip at the surface that has increased displacement and a more shallow dip angle as the depth increases.

The location and extent of the Waukesha fault has been variously interpreted. The length of the interpretations has varied from less than 40 miles to more than 133 miles. The current WGNHS interpretation, shown in Figure 13, gives a length of 82 miles with the downthrown sides nearest the Michigan Basin.

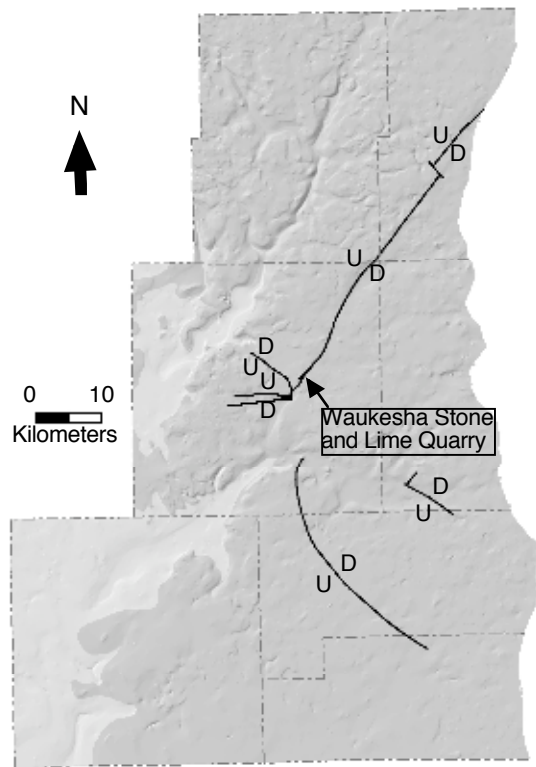


Figure 13. Map showing location of the Waukesha fault traces and the Waukesha Stone and Lime Quarry.

Waukesha Fault Quarry Description

The Waukesha Stone and Lime Quarry has been in operation for more than 150 years. It provides the most complete section of exposed Silurian rocks in southeastern Wisconsin (Kluessendorf and Mikulic, 1994). The Waukesha fault is exposed on the western edge of the quarry as shown in the air photo, Figure 14. Figure 15 is a photograph of this exposure. This photograph shows that the Waukesha fault exhibits hydrologic structures common to other fault systems (Caine, Evans and Forster, 1996; Rawling, Goodwin, and Wilson, 2001). A central fault core consisting of gouge and brecciated rock is surrounded on either side by damaged zones consisting of small splay fractures. The damaged zone is then surrounded by undamaged protolith. The fault core is approximately 10 feet in thickness and the damaged zones are between 5 and 10 feet in thickness.

This fault structure results in an increased vertical conductivity due to the fractured damaged zone and a decreased horizontal hydraulic conductivity due to the gouge in the fault

core. There are no measured values of the hydraulic conductivities for the core or damaged zone for the Waukesha fault in any of the formations it intersects. As a result, we used literature values of 5.6×10^{-3} ft/day and 0.28 ft/day to represent both the horizontal and vertical hydraulic conductivity of the fault. These values represent the range of reported fault core and damaged zones in Rawling and others (2001). These values may not adequately represent the core and damaged zones in the Maquoketa Formation but given the lack of Maquoketa specific data, they were used to represent a reasonable range.

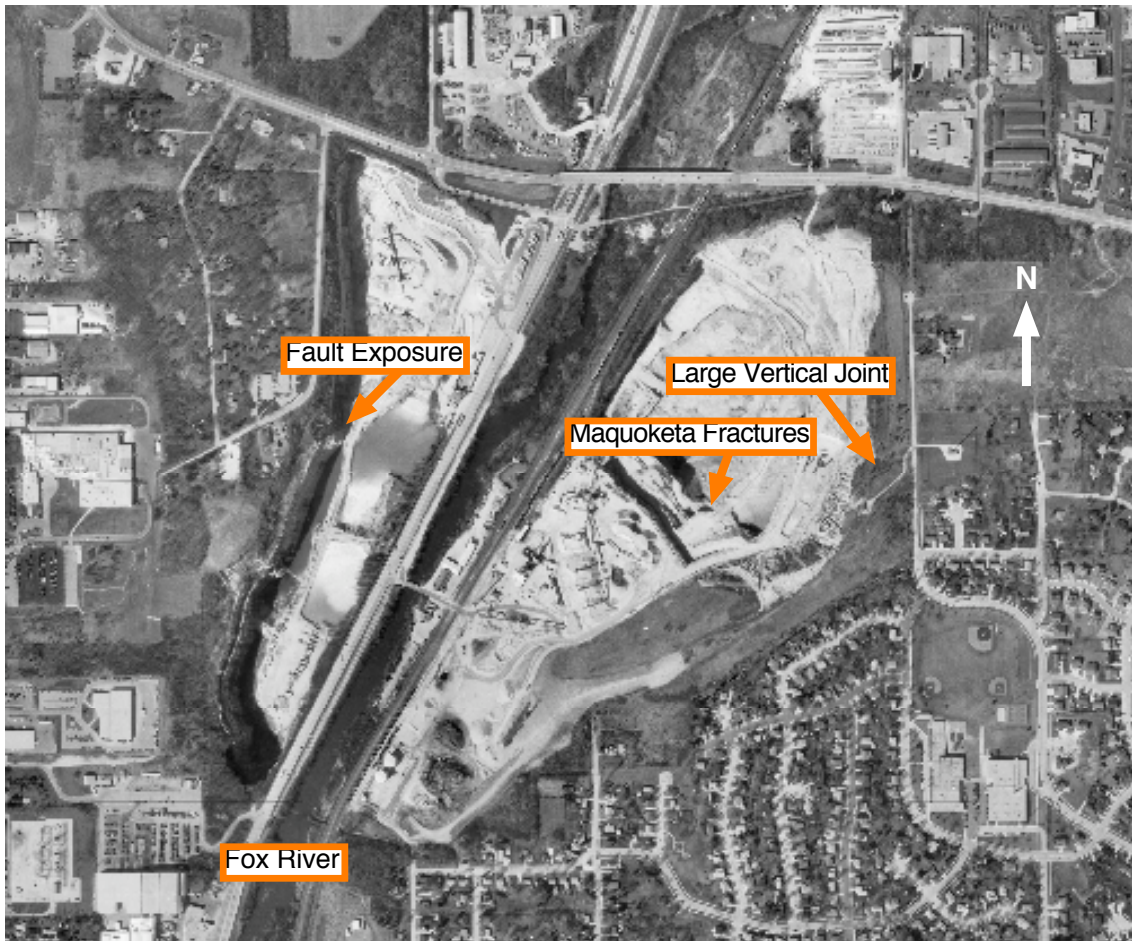


Figure 14. Air photo of the quarry and locations of the photographed fault exposure and fractures in quarry walls.

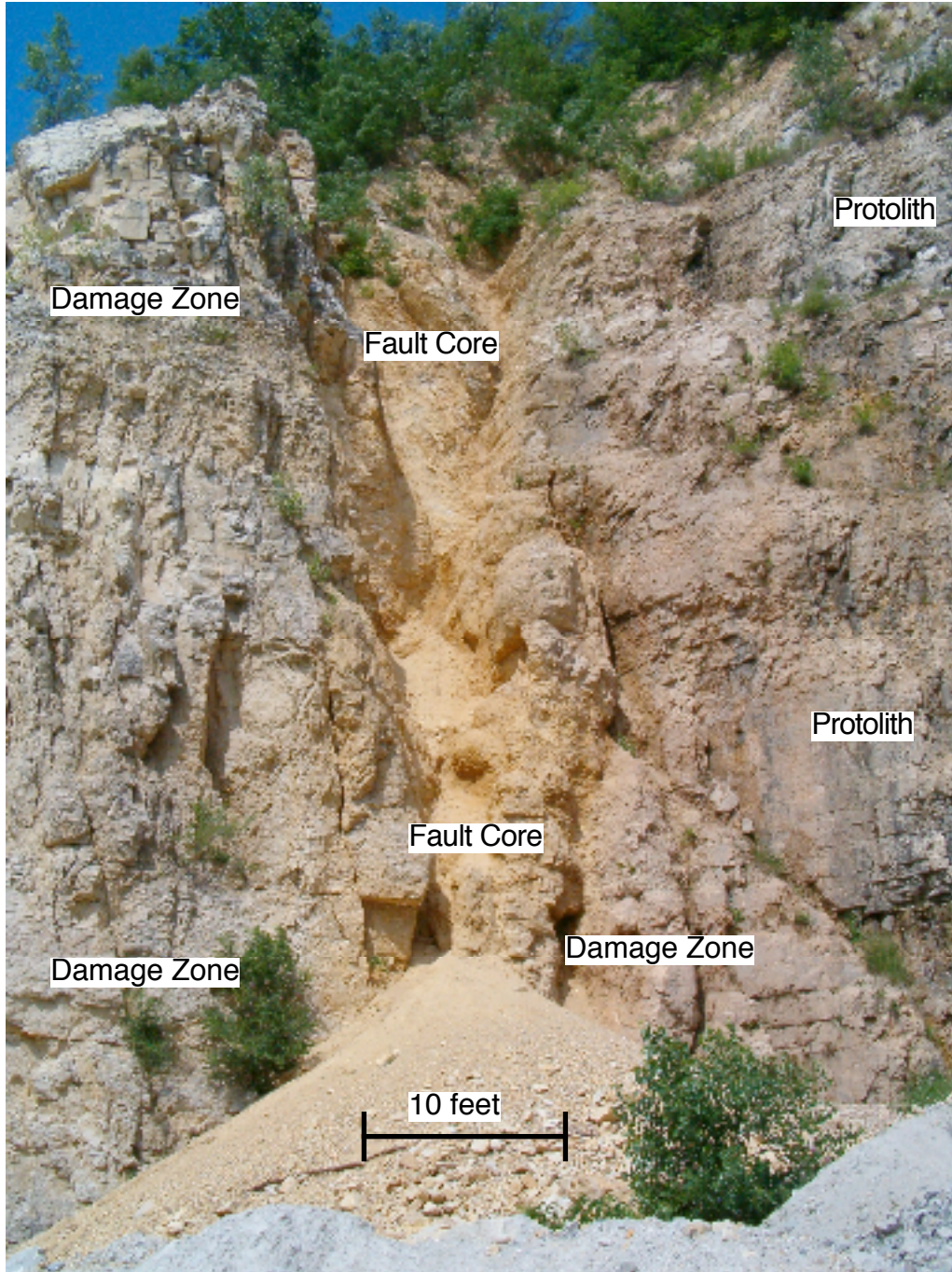


Figure 15. Photo of the Waukesha fault at the Waukesha Stone and Lime Quarry. The hydrologic features of the fault are labeled.

Waukesha Fault and regional groundwater flow model

We represented the Waukesha fault as identified by the WGNHS in the regional model by increasing the vertical hydraulic conductivity of the model cells that the fault intersected in the Maquoketa shale and Sinnipee dolomite. Although the model cells dimensions (2500 feet)

are large compared to the fault (10 feet), the hydraulic conductivity of the fault is orders of magnitude greater than the cell matrix hydraulic conductivity so that the fault is the main control on the average hydraulic conductivity of the combined cell and fault. The equivalent hydraulic conductivity analysis below treats the fault as a vertical plane that intersects the full thickness of a model cell. We assumed a simple vertically layered hydraulic conductivity zone model to calculate equivalent hydraulic conductivity for the model cells. The two end ranges of fault conductivity values of 5.6×10^{-3} ft/day and 0.28 ft/day were used in Equations 1a and b to calculate equivalent hydraulic conductivities for the model cells intersected by the assumed vertical plane of the fault.

$$Kv_{eq} = \frac{Kv_{cell}(L_{cell} - l_{fault}) + K_{fault}l_{fault}}{L_{cell}} \quad \text{eq 1a}$$

$$Kh_{eq} = \frac{L_{cell}}{\frac{L_{cell} - l_{fault}}{Kh_{cell}} + \frac{l_{fault}}{K_{fault}}} \quad \text{eq 1b}$$

where $L_{cell}=2500$ ft and $l_{fault}=10$ ft. Values of the fault conductivity (K_{fault}), model cell conductivities (Kh_{cell} and Kv_{cell}), and the calculated equivalent conductivities (Kh_{eq} and Kv_{eq}) are listed in Table 2 along with the corresponding lithologies/formations. This simple modeling shows that inclusion of the fault zone has less impact on the horizontal hydraulic conductivity than the vertical hydraulic conductivity, justifying the simple layer model treatment of the fault. The greatest change in the horizontal Kh occurs in the Silurian dolomite where a 10-foot thick fault zone with a conductivity of 5.6×10^{-3} ft/day decreases the horizontal hydraulic conductivity from 3.6 to 1 ft/day. In contrast, the greatest change in the vertical hydraulic conductivity is increased by orders of magnitude for a 10 ft thick fault zone with a hydraulic conductivity of 0.28 ft/day. The equivalent Kv of the Maquoketa shale is increased from 5.6×10^{-6} to 1.1×10^{-3} ft/day. For many of the lithologies, with the exception of the Maquoketa shale, the equivalent hydraulic conductivities are nearly identical to the model cell hydraulic conductivities. Following this reasoning, we simply modeled the fault zone as cells with the equivalent higher

hydraulic conductivities in the Maquoketa shale and the Sinnipee dolomite with the equivalent K_v 's shown below.

Table 2. Comparison between model cell and equivalent hydraulic conductivities/

Lithology/ Formation	K_{fault} (ft/day)	Kh_{cell} (ft/day)	Kh_{eq} (ft/day)	Kv_{cell} (ft/day)	Kv_{eq} (ft/day)
Silurian dolomite	0.28	1.00	0.99	1×10^{-3}	2.1×10^{-3}
Maquoketa shale	0.28	3.00×10^{-4}	3.01×10^{-4}	5×10^{-6}	1.1×10^{-3}
St Peter Sandstone	0.28	3.6	3.44	4×10^{-3}	5.1×10^{-3}
Silurian dolomite	5.6×10^{-3}	1.00	0.58	1×10^{-3}	1.0×10^{-3}
Maquoketa shale	5.6×10^{-3}	3.00×10^{-4}	3.01×10^{-4}	5×10^{-6}	2.7×10^{-5}
St Peter Sandstone	5.6×10^{-3}	3.6	1.01	4×10^{-3}	4.01×10^{-3}

For comparison to the base model without the fault, we conducted two model runs with the high (0.28 ft/day) and low (5.6×10^{-3} ft/day) estimates of the fault hydraulic conductivity. As can be seen from the model calibration statistics in Table 3, the low K fault does not significantly influence the model calibration, nor do large amounts of water pass through the fault in this model. The flow is only 0.4 mgd (277 gpm) over the entire length of the fault. The calibration statistics are significantly worse for the high conductivity fault. The residual mean is decreased to nearly -40 ft. This shows this model is overestimating heads in the deep sandstone aquifer as a result of large amounts of water flowing through fault. The absolute residual mean is also increased showing the model fit to the calibration targets is reduced. A third model run was conducted with the high (0.28 ft/day) fault conductivity and a lowered Maquoketa shale vertical hydraulic conductivity of 5×10^{-7} ft/day. This model, while it had better calibration statistics than the model with the high fault conductivity alone, was not an acceptable calibration.

Finally, a combined model run was made, similar to the one made for the multiaquifer wells. When combined with a high- K fault, reasonable changes to the deep sandstone aquifer ($Kh \times 3/4$ base), the Silurian dolomite ($Kh \times 1/2$ base), and the Maquoketa shale ($Kv \times 1/10$ base) are made, the residual mean is increased to 13.1 feet, meaning the model heads are now on average lower than the observed target heads. The absolute residual mean is at 36.3 feet. This set of sensitivity runs shows that it is possible to calibrate the regional model that includes the

Waukesha fault at the high conductivity estimate of 0.28 ft/day. If the Maquoketa shale Kv, the Silurian dolomite Kh or the deep sandstone aquifer Kh are increased closer to their base values from the combined model, the model fit will improve. These three parameters are all statistically correlated and so it is not possible to definitively state what combination of the three within the reasonable bounds used in the model will result in the absolute best model. The model does predict that the flow through the Waukesha fault at the high fault conductivity of 0.28 ft/day will be around 4 mgd. This value is similar to the predicted flow through the combined best-fit multiaquifer well model. This similarity should perhaps have been anticipated because both models allow additional flow through the Maquoketa shale over a distributed areal extent.

Table 3. Model fit statistics between groundwater flow models.

Model Name	Residual Mean (ft)	Absolute Residual Mean (ft)	Downward Flow through the fault (mgd)
Base (no fault included)	1.7	29.4	--
Fault K=0.0056 ft/day	0.9	29.7	0.4
Fault K=0.28 ft/day	-39.5	50.7	3.2
Fault K=0.28 ft/day Maquoketa K=5x10 ⁻⁷ ft/day	-21.6	42.8	3.6
Fault K=0.28 ft/day Deep SS x 3/4 Silurian Dolomite x 1/2	-7.8	35.3	3.4
Fault K=0.28 ft/day Deep SS Kh x 3/4 Silurian Dolomite Kh x 1/2 Maquoketa Kv x 1/10	13.1	36.3	3.9

Waukesha Fault Summary

We conducted a study of the Waukesha fault system by conducting a literature review, a site visit to the only known exposure of the fault, and by including the fault in the regional model for southeastern Wisconsin. The literature review showed that the fault is known only through displacements in well logs and associated gravity and magnetic signatures. The extent of the fault is not well known and will likely be reinterpreted as more well data become available.

The only exposure of the Waukesha fault system in the Waukesha Stone and Lime Quarry showed that in the Silurian dolomite, the Waukesha fault exhibits a hydrologic structure common other faults. In the quarry, the fault is near vertical with a fault core consisting of gouge and breccia surrounded on either side by a damaged zone of near vertical splay faults. The total width of the fault zone is only 15 to 20 feet. It is unknown whether or not this fault structure is present in the Maquoketa shale.

The modeling effort showed that inclusion of the fault with a horizontal and vertical hydraulic conductivity less than 5.6×10^{-3} ft/day does not significantly affect the model calibration nor is there significant flow through the fault, less than 0.5 mgd. When the fault conductivity is increased to 0.28 ft/day, the model calibration is no longer acceptable. Similar to the multiple aquifer well sensitivity runs, it is not possible to calibrate the model by varying a single parameter. For example, decreasing the Maquoketa shale hydraulic conductivity alone but within reasonable bounds does not give a calibrated model. However, a combination of decreasing the Maquoketa shale K_v , the deep sandstone K_h , and the Silurian K_h could be found that will give a reasonable fit. The approximate discharge through the Waukesha fault, assuming a high fault conductivity of 0.28 ft/day is around 4 mgd. This value is significant but is not the dominant flow across the Maquoketa shale.

Other Faults and Joints

The Waukesha fault is present and does conduct some amount of water. However, we suspect that faults, joints, and fractures are ubiquitous throughout the Maquoketa Formation in southeastern Wisconsin and that they contribute most of the flow across the Maquoketa shale. Few of these fractures are needed to allow sufficient flow (Hart and others, 2005). During our site visit to the Waukesha Stone and Lime Quarry, we photographed several other potential joints and fractures shown in Figures 16 and 17. The locations of the photographs below are shown in Figure 14. These are not the only fractures and joints observed in the quarry and so it seems unlikely that they are the only ones present in the Maquoketa throughout southeastern Wisconsin. Further study might be able to identify whether or not the fracture in Figure 16 was caused by excavation and blasting or if it was present prior to development of the quarry. The large joint shown in Figure 17 is too large and well developed to have been caused by blasting.

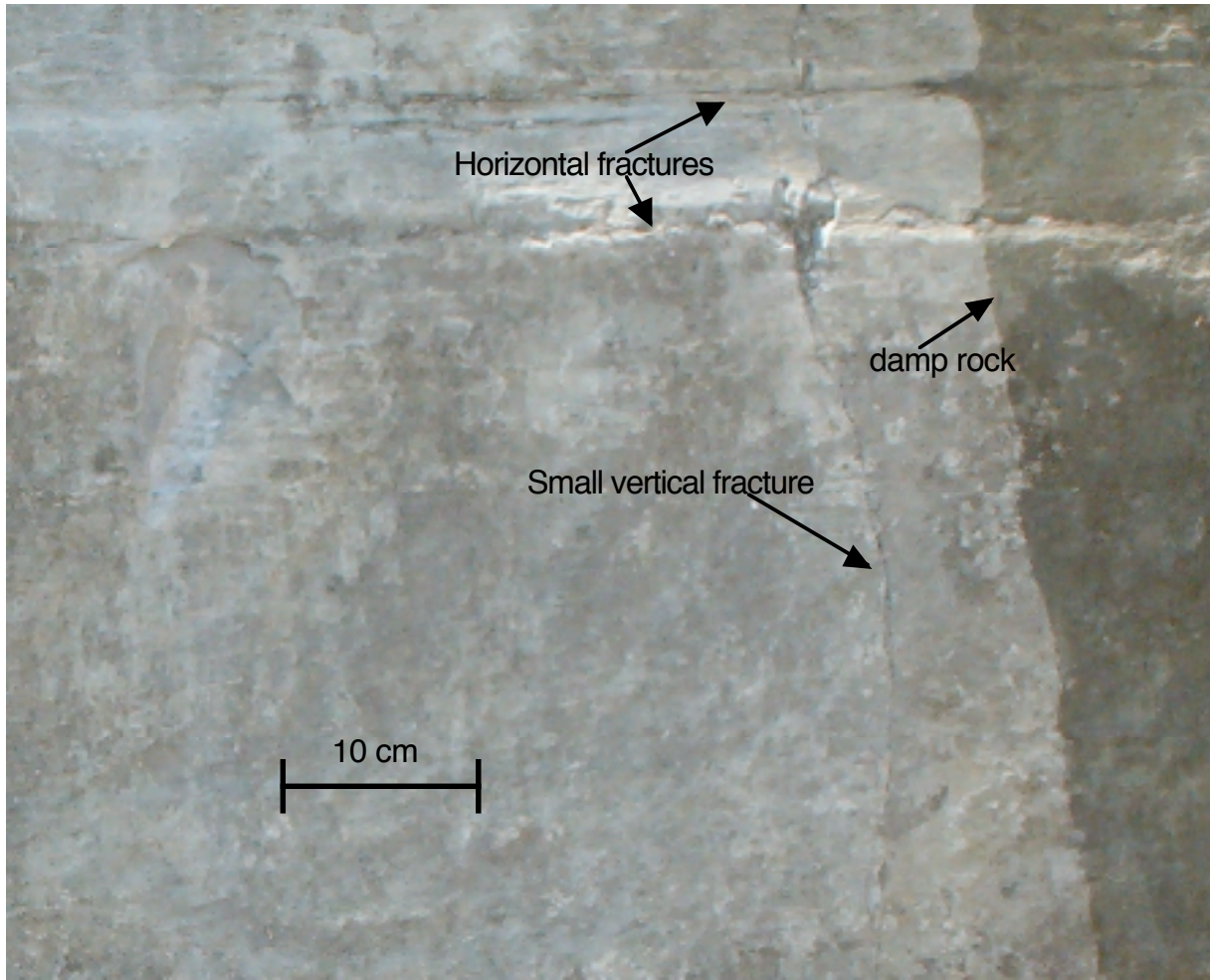


Figure 16. Photo of fractures in the upper Maquoketa Formation in the Waukesha Stone and Lime Quarry.



Figure 17. Joint in the east quarry of the Waukesha Lime and Stone Quarry.

Redevelopment of the Pewaukee Corehole

A last phase of this project was to rehabilitate a corehole previously used in studies of the Maquoketa shale (Eaton and others, 2000; Eaton and Bradbury, 2003, Hart and others, 2005)

and conduct short interval slug tests in the corehole. We attempted to remove the Solinst packer string used in previous studies. The packer string failed and we were unable to easily remove it. We had to resort to overdrilling the corehole with an air rotary drill rig. This technique rehabilitated the well so that it was available for additional study. Drill cuttings showing the ground residuum of the packer string, air-lines, and transducer cables is shown in Figure 18.

We conducted a short interval packer test in the rehabilitated well but found that the hydraulic conductivity of the Maquoketa shale was too low for conventional packer testing. The heads in the 1-inch diameter packer string standpipe did not decrease over a 12-hour period. We plan to design a shut-in confined system that will have significantly less storage than the traditional standpipe. That smaller storage will decrease the amount of water that must flow and the time needed to reach equilibrium. This project brought forth the need for us to develop this type of system.



Figure 18. Cuttings showing ground-up packer.

We also compared the heads in the buried transducers from wells placed near this site in a previous study (Eaton and others, 2000). Figure 19 shows the heads from April 2000 within two months of installation of the buried vibrating wire transducers and from June 2006. There has been little change except in the interval at 275 feet depth where the head in the buried transducer

had decreased by 13 feet.

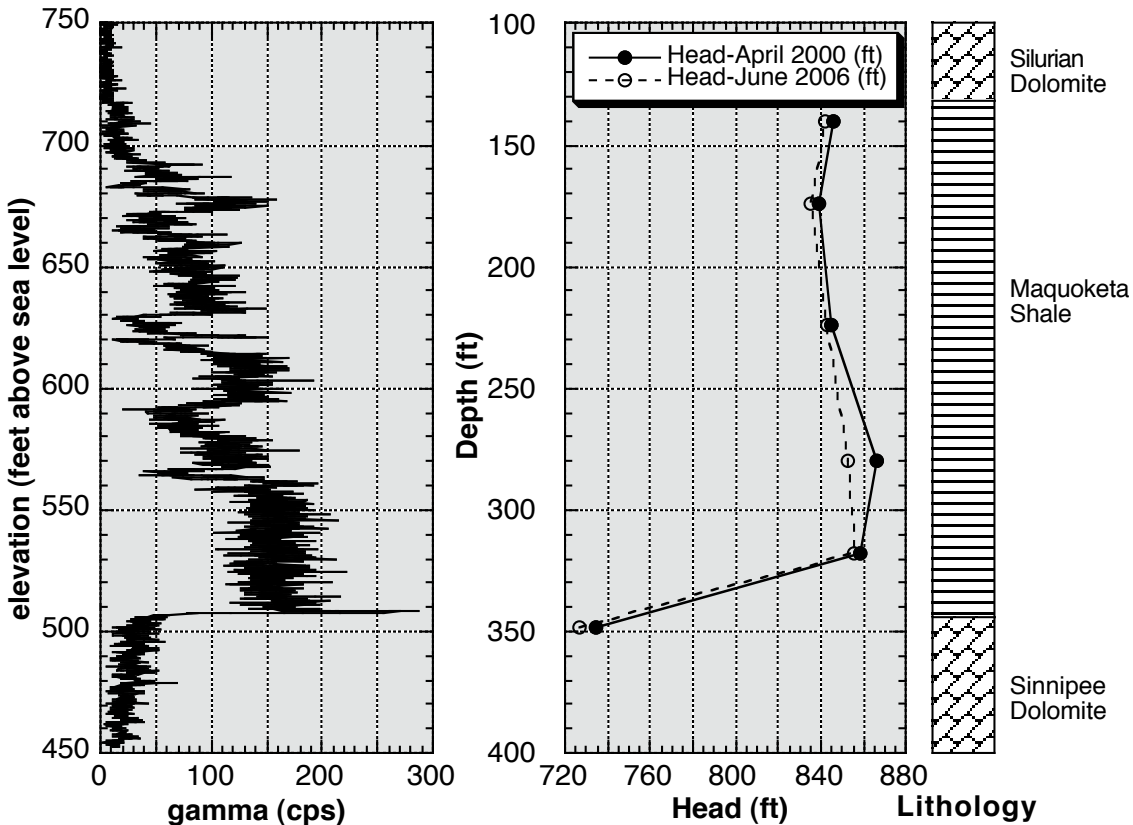


Figure 19. Water levels in the buried piezometer nest.

These data presented a puzzle in June 2000 and they still present a puzzle. It is not certain how the highest head in the section can be in the aquitard. Though several theories have been presented, none is satisfactory. Those theories include that the high heads are left from predevelopment time and the head decrease in the deep sandstone aquifer has not yet had time to diffuse upward. Another possible explanation is that the lines of constant head are curved due to the presence of the shale aquitard in a manner presented by Freeze and Witherspoon, 1967. The vertical head profile in Figure 19 would be similar to one taken from beneath the arrow in Figure 20. At the surface the heads would be at an intermediate value, increase to a maximum at the top of the aquitard and then decrease dramatically in and beneath the aquitard. Other explanations for the head profile shown in Figure 19 include chemically induced head potentials or simply a misplacement of the transducer. We plan to revisit this site to gather additional data so that some of these theories may be eliminated.

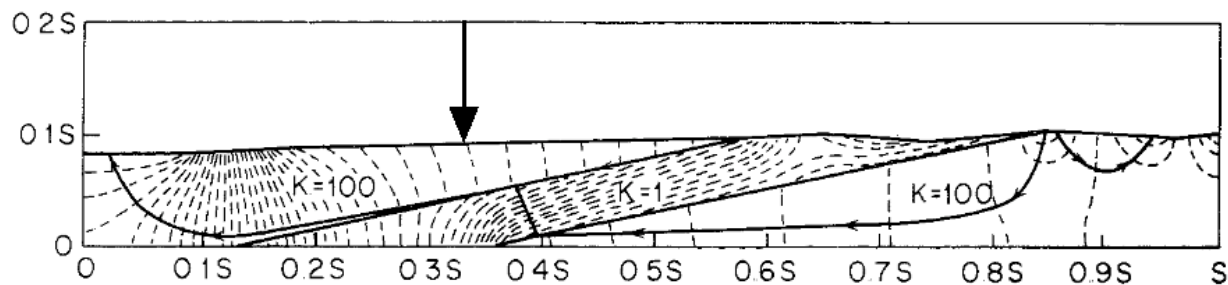


Figure 20. The effect of an aquitard in a regional flow system (after Freeze and Witherspoon, 1967). The dashed lines are hydraulic head contours.

Summary

The Maquoketa Formation forms a regional aquitard in southeastern Wisconsin. This aquitard controls much of the flow in the deep sandstone aquifer. Understanding the pathways of flow through the Maquoketa Formation that allow contaminants and recharge to enter the deep sandstone aquifer is essential for protection of the aquifer and quantifying the groundwater flow system.

We studied two pathways, flow through multiaquifer wells and flow through the Waukesha fault system. The modeled flow through the multiaquifer wells is 4.4 mgd. Model calibration at higher flows is not possible without adjusting hydrologic parameters outside of a reasonable bound. The distribution of flows through the multiaquifer wells shows that less than half of the wells provide nearly 90 percent of the flow. This will allow the WDNR to target the highest flow wells for abandonment and prevent contamination of the deep sandstone aquifer. Abandonment of the multiaquifer wells will result in increased drawdown in the deep sandstone aquifer as this source of recharge is eliminated. This effect will be small because the flow rate of 4.4 mgd is only 15 percent of the total pumped from the deep sandstone aquifer and because many of the wells may never be located for abandonment.

Flow through the Waukesha fault system was investigated. If the lower estimate for the fault hydraulic conductivity of 5.6×10^{-3} ft/day is correct, then the Waukesha fault plays a relatively unimportant role in the larger flow system. If the hydraulic conductivity is closer to the upper estimate of 0.28 ft/day, the flow through the Waukesha fault of around 4 mgd is similar in magnitude to that through the multiaquifer wells. As was the case with the multiaquifer wells, model calibration at higher flows is not possible without adjusting hydrologic parameters outside

of their reasonable bounds. While the flow value of 4 mgd is significant, it does not represent the majority of flow across the Maquoketa Formation. We suspect many faults, fractures and joints contribute to flow. Evidence of some of these additional joints and fractures was observed in the Waukesha Lime and Stone Quarry.

In summary, multiaquifer wells and the Waukesha fault may transmit significant flow through the Maquoketa Formation but they do not dominate the flow system. Rather we suspect many distributed joints and fractures transmit most of the flow through the Maquoketa Formation. The number of multiaquifer wells has been reduced in the last two decades. This had led to a decrease of flow through these wells that helped replenish the deep sandstone aquifer. However, abandonment of these wells should be pursued with some attention paid to the consequences of reduced flow to the deep sandstone aquifer. The Waukesha fault might contribute significant flow if the hydraulic conductivity in the fault is dominated by fractures in a damaged zone through the Maquoketa Formation. Otherwise, the flow through the Waukesha fault likely is not significant and it is merely one of many fractures and joints that transmit water across the Maquoketa Formation.

Recommendations

- Continue abandonment of the multiaquifer wells. They do not contribute enough water to the deep sandstone aquifer to offset the risk of contaminants entering the deep sandstone aquifer through these wells.
- Additional observation wells should be placed in the deep sandstone aquifer, ideally at discrete depths rather than being open to the entire deep sandstone aquifer. The calibration effort was hampered by a lack of water level observations both with depth and areally across southeastern Wisconsin. We were unable to differentiate between the different pathways, in part, because of this lack of data.
- Collect groundwater use data for high capacity active wells. Only 69 of the 172 multiaquifer wells had pumping records available. The overall water use is one of the more important but less well known parameters in the regional flow model. For purposes of this effort, decadal or yearly records would have been sufficient.

- Continue tracking the status of the high capacity wells. Multiaquifer wells present a pathway for contaminants to enter the deep sandstone aquifer. Unreported and unabandoned wells may present an unknown pathway for contaminants to enter the deep sandstone aquifer.

References

- Braschayko, S.M., 2005, The Waukesha Fault and Its Relationship to the Michigan Basin: A Literature Compilation. (In submission) Wisconsin Geological and Natural History Survey Open File Report.
- Caine, S.C., J.P. Evans, and C.B. Forster, 1996, Fault zone architecture and permeability structure, *Geology*, v. 24, no. 11, p. 1025-1028.
- Dunning, C P, D.T. Feinstein, R.J. Hunt, J.T. Krohelski, 2004, Simulation of ground-water flow, surface-water flow, and a deep sewer tunnel system in the Menomonee Valley, Milwaukee, Wisconsin., Publications of the U. S. Geological Survey, Report: SIR 2004-5031, 40 pp. Reston, VA.
- Eaton, T. T., Hart, D.J., Bradbury, K.R., and Wang, H.F. 2000. Hydraulic Conductivity and Specific Storage of the Maquoketa Shale. Madison, Wisconsin: University of Wisconsin Water Resources Institute, 2001 <http://digital.library.wisc.edu/1711.dl/EcoNatRes.WRIGRR01-01>.
- Eaton, T. T, K.R. Bradbury, 2003, Hydraulic transience and the role of bedding fractures in a bedrock aquitard, southeastern Wisconsin, USA, *Geophysical Research Letters*, vol.30, no.18, 4 pp.
- Evans, T.J. and R.M. Peters, Roger, 2003, The challenge of mapping what can't be seen; a preliminary geologic map of the bedrock surface of southeastern Wisconsin, *Abstracts with Programs - Geological Society of America*, vol.35, no.6, pp.68.
- Feinstein, D.T., T.T. Eaton, D.J. Hart, J.T. Krohelski, K.R. Bradbury, 2005, A Regional Aquifer Model for Southeastern Wisconsin, Technical Report 41, Southeastern Wisconsin Regional Planning Commission.
- Freeze, R.A. and P.A. Witherspoon, 1967, Theoretical analysis of regional groundwater flow: 2. Effect of water-table configuration and subsurface permeability variation. *Water Resources Research*, 3, pp. 623-634.
- Gotkowitz, M.B., 2006, Personal communication.
- Halford, K.J. and R.T. Hanson, 2002, User Guide for the Drawdown-Limited, Multi-Node Well (MNW) Package for the U.S. Geological Survey's Modular Three-Dimensional Finite-Difference Ground-Water Flow Model, Versions MODFLOW-96 and MODFLOW-2000, U.S.G.S. Open File Report 02-293, Sacramento, California.
- Hanson, R.T., P. Martin, K.M. Kocot, 2002, Simulation of Ground-water/surface-water flow in the Santa Clara-Calleguas ground-water basin, Ventura County, California: U.S. Geological Survey Water Resources-Investigations Report WRIR 02-4136.
- Hart, D.J., K.R. Bradbury, D.T. Feinstein, 2005, The vertical hydraulic conductivity of an aquitard at two spatial scales. *Ground Water*, Volume 44, Issue 2, Page 201-211.
- Kluessendorf, J. and D.G. Mikulic, 1994, Stop 7A and 7B, Waukesha Lime and Stone Company Quarries, Waukesha, Wisconsin in *"Guidebook to the Problems Associated with Artesian*

- Systems and Land-usage in Southeastern Wisconsin*” AAPG Annual Fall Geology Field Conference.
- Nelson, K.G., 1977 A Guidebook for the 41st Annual Tri-State Field Conference. University of Wisconsin-Milwaukee.
- Randolph, L.C. 1991, The effects of faults on the groundwater system in the Hickory Sandstone aquifer in central Texas. Master’s Thesis, Texas A&M University, College Station, TX.
- Rawling, G.C., L.B. Goodwin, and J.L. Wilson, 2001, Internal arch tecture, permeability structure, and hydrologic significance of contrasting fault-zone types, *Geology*, v. 29, no. 1 p. 43-36.
- Rovey, C.W. and D.S. Cherkauer, 1994, Relation between hydraulic conductivity and texture in a carbonate aquifer; regional continuity, *Ground Water*, vol.32, no.2, pp.227-238.
- J. D. Skalbeck, Couch, J.N., Helgesen, R.S., and Swosinski, D.S., 2006, Coupled Modeling of Gravity and Aeromagnetic Data to Estimate Subsurface Basement Topography in Southeastern Wisconsin, *Geoscience Wisconsin*, pp. 53-64.
- Sverdrup, K.A., Kean, W.F., Herb, S., and Brukard, S.A. 1997 Gravity Signature of the Waukesha Fault, Southeastern Wisconsin. *Geoscience Wisconsin*, Vol. 16, pp 47-54.

Appendix B. Table of multiaquifer wells.

Darker shading denotes wells with a higher potential for cross aquifer flow.

WGNHS Id	County	Well Name	WUWN	Status	Year Completed	Year Abandoned	Down Flow (gpm)	Flow Potential
140044	Dodge		BF620	Present	1948		0	Low
140199	Dodge			Present	1965		2	Low
300001	Kenosha			Present	1946		34	High
300002	Kenosha			Abandoned	1920	2000	1	None
300008	Kenosha			Present	1906		3	Low
300012	Kenosha			Present	1945		47	High
300042	Kenosha			Present	1948		7	Low
300183	Kenosha			Present	1948		5	Low
300261	Kenosha			Present	1963		21	High
300262	Kenosha			Present	1963		2	Low
300286	Kenosha			Present	1965		24	High
300343	Kenosha			Present	1981		0	Low
300344	Kenosha			Present	1981		0	Low
300360	Kenosha		HU123	Reconstructed	1987		114	None
300739	Kenosha			Present	1966		3	Low
300758	Kenosha			Present	1969		6	Low
300850	Kenosha			Present	1976		2	Low
300853	Kenosha			Present	1962		2	Low
300929	Kenosha			Present	1964		2	Low
301122	Kenosha			Present	1987		66	High
410003	Milwaukee	Chicago & NW Railroad		Inactive	1910		83	Very High
410005	Milwaukee	Chicago & NW Railroad		Inactive	1920		84	Very High
410007	Milwaukee	Brown Deer Park	BA143	Reconstructed	1935		359	None
410010	Milwaukee	Greenebaum tanning Co.		Present	1937		37	High
410011	Milwaukee	Square D Company		Abandoned	1941	2001	0	None
410016	Milwaukee	Wauwatosa City Well #5		Abandoned	1928	Unknown	81	None
410017	Milwaukee	Wauwatosa City Well #6		Abandoned	1930	Unknown	33	None
410018	Milwaukee	Wauwatosa City Well #7		Abandoned	1939	Unknown	37	None

WGNHS Id	County	Well Name	WUWN	Status	Year Completed	Year Abandoned	Down Flow (gpm)	Flow Potential
410020	Milwaukee	Miller Brewing		Abandoned	1933	2002	3	None
410022	Milwaukee	Allis Chalmers	BE695	Abandoned	1937	2000	6	None
410024	Milwaukee	Milky Way Custard		Inactive	1929		62	High
410025	Milwaukee	Harnishfeger Corp.		Abandoned	1942	2000	56	None
410032	Milwaukee	Kearney and Trecker Co.		Present	1941		47	High
410034	Milwaukee	Bronson Manor Well #2		Inactive	1946		44	High
410035	Milwaukee	A.O. Smith Corp.		Present	1937		0	Low
410038	Milwaukee	Bowling Central		Inactive	1940		2	Low
410039	Milwaukee	A.O. Trostel Tanning Co.		Abandoned	1937	1976		None
410040	Milwaukee	Schlitz Brewery		Present	1934		20	Moderate
410041	Milwaukee	Schlitz Brewery		Abandoned	1937	Unknown	20	None
410043	Milwaukee	Premier Pabst Corp.		Inactive	1937		43	High
410046	Milwaukee	Boston Store Well		Reconstructed	1936	2003	15	None
410047	Milwaukee	Woolworth Store Well		Present	1937		14	Moderate
410048	Milwaukee	Plankinton N Arcade		Inactive	1937		14	Moderate
410049	Milwaukee	Medford Hotel		Present	1937		0	Low
410051	Milwaukee	Pittsburgh Plate Glass		Inactive	1939		16	Moderate
410052	Milwaukee	Zinn Malting Co.	BE717	Abandoned	1947	1997	3	None
410055	Milwaukee	Tower Theater		Present	1939		29	High
410058	Milwaukee	Eagles Club		Abandoned	1939	2001	32	None
410064	Milwaukee	Wehr Steel Co.		Present	1942		24	High
410075	Milwaukee	Rundle Manufacturing		Inactive	1941		17	Moderate
410077	Milwaukee	Forest Home Cemetary #4		Active	1946		3	Low
410080	Milwaukee	Maynard Electric	BE707	Abandoned	1943	2001	21	None
410081	Milwaukee	Crucible-Steel casting Co.	BE720	Abandoned	1943	1991	3	None
410083	Milwaukee	Mueller Furnace Co. #2		Inactive	1941		0	Low
410089	Milwaukee	Ladish Drop Forge Co.		Abandoned	1941	2004	47	None
410093	Milwaukee	Milwaukee Co. Park		Present	1932		49	High

WGNHS Id	County	Well Name	WUWN	Status	Year Completed	Year Abandoned	Down Flow (gpm)	Flow Potential
410098	Milwaukee	Le Roi Company		Inactive	1944		45	High
410099	Milwaukee	Wisconsin Motor Corp.		Inactive	1941		40	High
410100	Milwaukee	Krause Milling		Inactive	1938		34	High
410102	Milwaukee	Globe Steel Tubes		Present	1898		13	Moderate
410103	Milwaukee	Globe Steel Tubes #2	BE696	Inactive	1940		13	Moderate
410105	Milwaukee	Kurth Malting #3		Present	1941		13	Moderate
410106	Milwaukee	Froedert Grain and Malting	BE699	Active	1928		13	Moderate
410107	Milwaukee	Froedert Grain and Malting #2	BE700	Active	1938		13	Moderate
410124	Milwaukee	Good Hope Cemetery		Abandoned	1940	2005	50	None
410132	Milwaukee	White Manor Park		Inactive	1942		30	High
410133	Milwaukee	American Metal Products		Abandoned	1940	2004	0	None
410145	Milwaukee	Varsity Theatre Well		Inactive	1937		1	Low
410153	Milwaukee	Lakeside Lab/Badger Meter		Abandoned	1947	1993	90	None
410224	Milwaukee	Red Star Yeast		Present	1948		38	High
410225	Milwaukee	Wehr Steel Co. Well #2		Abandoned	1948	1991	53	None
410227	Milwaukee	Krause Milling/Kurth Malting		Inactive	1937		5	Low
410233	Milwaukee	Bronson Manor Well #3		Inactive	1948		49	High
410285	Milwaukee	Luickuice Cream		Present	1950		37	High
410287	Milwaukee	Second Home Cemetery		Inactive	1949		54	High
410294	Milwaukee	McClymon Marble/Thiele Tanning Co.		Abandoned	1925	2004	0	None
410299	Milwaukee	Milwaukee Western Malt		Inactive	1937		3	Low
410315	Milwaukee	Bay Shore Shopping Center		Present	1953		20	High
410324	Milwaukee	Great Atlantic and Pacific Tea		Inactive	1954		55	High
410326	Milwaukee	Kurth Malting #4	BE705	Inactive	1954		13	Moderate
410330	Milwaukee	Oak Creek Station #2		Present	1953		27	High
410331	Milwaukee	Oak Creek Station #1		Abandoned	1953	1980		None
410341	Milwaukee	Bay Shore Shopping Center #2		Inactive	1954		46	High

WGNHS Id	County	Well Name	WUWN	Status	Year Completed	Year Abandoned	Down Flow (gpm)	Flow Potential
410356	Milwaukee	File and Stowell		Inactive	1937		20	High
410361	Milwaukee	Blatz Brewing		Inactive	1935		3	Low
410378	Milwaukee	Wauwatosa City Well #11		Abandoned	1955	Unknown	106	None
410383	Milwaukee	Towne Realty Co.		Inactive	1955		14	Moderate
410396	Milwaukee	Hales happiness subdivision		Active	1977		27	High
410400	Milwaukee	Security Acres subdivision	BG441	Abandoned	1956	2001	64	None
410406	Milwaukee	U.s. Army antiaircraft facility		Abandoned	1956	2000	39	None
410408	Milwaukee	U.s. Army antiaircraft facility		Inactive	1956		33	High
410410	Milwaukee	Hales happiness subdivision		Active	1956		52	High
410413	Milwaukee	U.s. Army antiaircraft facility		Abandoned	1956	date unknown	30	None
410416	Milwaukee	Pelham Heath subdivision	FX306	Abandoned	1956	2000	62	None
410417	Milwaukee	Joint School District Well		Present	1956		29	High
410420	Milwaukee	Evert Container Corp.		Abandoned	1956	1994	101	None
410431	Milwaukee	Badger Meter		Abandoned	1957	1993	84	None
410435	Milwaukee	Regal Manor subdivision		Present	1957		51	High
410468	Milwaukee	Glendale Gardens		Present	1959		14	Moderate
410472	Milwaukee	Schroedel construction/Security Acres		Present	1960		32	High
410492	Milwaukee	Milwaukee Tallow and Grease	BE718	Abandoned	1961	2001	3	None
410493	Milwaukee	South Gate Manor		Present	1960		42	High
410494	Milwaukee	Franklin High School	DK828	Abandoned	1962	1998	51	None
410504	Milwaukee	Mt. Carmel Nursing Home		Abandoned	1963	1968		None
410560	Milwaukee	John Edwards/Town View subdivision		Present	1942		55	High
410571	Milwaukee	Whitnall middle School		Present	1970		45	High
411039	Milwaukee	Donald Woelbing		Present	1986		0	Low
460027	Ozaukee		BG645	Active	1956		0	Low
460039	Ozaukee		BG652	Active	1958		1	Low
460048	Ozaukee			Abandoned	1971	Unknown	25	None

WGNHS Id	County	Well Name	WUWN	Status	Year Completed	Year Abandoned	Down Flow (gpm)	Flow Potential
460073	Ozaukee		BG631	Reconstructed	1963		67	None
460078	Ozaukee		BG646	Active	1965		6	Low
460079	Ozaukee		BG653	Active	1965		0	Low
460089	Ozaukee		BG647	Active	1967		0	Low
460357	Ozaukee			Active	1969		25	High
520013	Racine			Present	1928		57	High
520015	Racine		BH155	Abandoned	1918	1982		None
520017	Racine			Abandoned	1939	2005	73	None
520022	Racine			Present	1910		33	High
520023	Racine	Wisconsin Natural Gas Co.		Abandoned	1929	1970		None
520024	Racine			Present	1937		19	Moderate
520028	Racine			Present	1940		0	Low
520035	Racine		BG735	Present	1932		0	Low
520040	Racine			Abandoned	1910		18	None
520047	Racine			Present	1955		55	High
520048	Racine		BG747	Abandoned	1955		61	None
520049	Racine			Present	1956		40	High
520053	Racine			Present	1957		65	High
520060	Racine			Abandoned	1959	1993	46	None
520141	Racine			Present	1959		14	Moderate
520142	Racine			Present	1957		14	Moderate
520240	Racine			Present	1960		6	Low
520315	Racine			Present	1899		39	High
520353	Racine			Present	1966		20	High
520371	Racine			Present	1971		32	High
520399	Racine			Present	1985		25	High
520447	Racine		LN982	Present	1997		2	Low
520676	Racine			Present	1966		28	High

WGNHS Id	County	Well Name	WUWN	Status	Year Completed	Year Abandoned	Down Flow (gpm)	Flow Potential
520765	Racine			Present	1979		14	Moderate
521515	Racine			Present	1964		14	Moderate
650538	Walworth			Present	1965		12	Moderate
651095	Walworth			Present	1973		1	Low
651252	Walworth			Abandoned	1994	1994	0	None
651253	Walworth			Present	1992		1	Low
651262	Walworth			Present	1987		2	Low
670006	Washington			Present	1946		22	High
670149	Washington		BH257	Present	1968		3	Low
670415	Washington			Present	1968		57	High
670797	Washington		BH247	Present	1975		0	Low
680002	Waukesha			Present	1944		68	High
680004	Waukesha		BH401	Abandoned	1931	2001	0	None
680145	Waukesha			Reconstructed	1964		86	None
680154	Waukesha			Present	1957		64	High
680163	Waukesha			Present	1958		0	Low
680214	Waukesha			Present	1962		78	Very High
680707	Waukesha			Present	1968		0	Low
680754	Waukesha			Present	1966		68	High
680957	Waukesha			Present	1970		50	High
681102	Waukesha			Present	1973		56	High
681105	Waukesha			Present	1972		3	Low
681294	Waukesha			Present	1985		0	Low
682315	Waukesha		DD543	Present	1989		57	High
682336	Waukesha			Present	1972		2	Low
682347	Waukesha			Present	1977		86	Very High
682352	Waukesha			Present	1956		119	Very High
682421	Waukesha			Present	1978		0	Low

WGNHS Id	County	Well Name	WUWN	Status	Year Completed	Year Abandoned	Down Flow (gpm)	Flow Potential
682554	Waukesha		GF696	Present	1993		0	Low
682603	Waukesha		AC164	Present	1988		3	Low
682606	Waukesha			Present	1987		0	Low
682639	Waukesha			Abandoned	1977	1997	87	None